frontiers in Marine Science

ORIGINAL RESEARCH
published: 14 December 2017
doi: 10.3389/fmars.2017.00410

Abyssal Solenogastres (Mollusca, Aplacophora) from the Northwest Pacific: Scratching the Surface of Deep-Sea Diversity Using Integrative Taxonomy

Franziska S. Bergmeier[1], Angelika Brandt[2], Enrico Schwabe[3] and Katharina M. Jörger[1,3]*

[1] Systematic Zoology, Faculty of Biology, Department II, Ludwig-Maximilians-Universität München, Munich, Germany,
[2] Department of Marine Zoology, Senckenberg Research Institute and Natural History Museum, Frankfurt am Main, Germany,
[3] Section Mollusca, SNSB-Bavarian State Collection of Zoology, Munich, Germany

OPEN ACCESS

Edited by:
Chong Chen,
Japan Agency for Marine-Earth Science and Technology, Japan

Reviewed by:
Emanuel Redl,
University of Vienna, Austria
Hiroshi Saito,
National Museum of Nature and Science, Japan

***Correspondence:**
Franziska S. Bergmeier
franzi.bergmeier@gmail.com

Specialty section:
This article was submitted to Marine Evolutionary Biology, Biogeography and Species Diversity, a section of the journal Frontiers in Marine Science

Received: *29 September 2017*
Accepted: *30 November 2017*
Published: *14 December 2017*

Citation:
Bergmeier FS, Brandt A, Schwabe E and Jörger KM (2017) Abyssal Solenogastres (Mollusca, Aplacophora) from the Northwest Pacific: Scratching the Surface of Deep-Sea Diversity Using Integrative Taxonomy. Front. Mar. Sci. 4:410. doi: 10.3389/fmars.2017.00410

Solenogastres (Aplacophora) is a small clade of marine, shell-less worm-molluscs with close to 300 valid species. Their distribution ranges across all oceans, and whereas the vast majority of species has been collected and described from the continental shelf and slope, only few species are known from depths below 4,000 m. Following traditional taxonomy, identification of specimens to species level is complex and time-consuming and requires detailed investigations of morphology and anatomy—often resulting in the exclusion of the clade in biodiversity or biogeographic studies. During the KuramBio expedition (Kuril-Kamchatka Biodiversity Studies) to the abyssal plain of the Northwest Pacific and the Kuril-Kamchatka Trench, 33 solenogaster specimens were sampled from 4,830 m to 5,397 m. Within this study we present an efficient workflow to address solenogaster diversity, even when confronted with a high degree of singletons and minute body sizes, hampering the use of single individuals for multiple morphological and molecular approaches. We combine analyses of external characters and scleritome with molecular barcoding based on a self-designed solenogaster specific set of mitochondrial primers. Overall we were able to delineate at least 19 solenogaster lineages and identify 15 species to family level and beyond. Based on our approach we identified three key lineages from the two regionally most species-rich families (Acanthomeniidae and Pruvotinidae) for deeper taxonomic investigations and describe the novel abyssal species *Amboherpia abyssokurilensis* sp. nov. (Cavibelonia, Acanthomeniidae) using microanatomical 3D-reconstructions. Our study more than doubles the previous records of solenogaster species from the Northwest Pacific and its marginal seas. Almost all lineages are reported for the first time from the region of the (Northwest) Pacific, vastly expanding distribution ranges of the respective clades. Moreover it doubles the number of Solenogastres collected from abyssal depths on a global scale and underlines the lack of exploratory α-diversity work in the abyssal zone for reliable species estimates in marine biodiversity.

Keywords: biodiversity, molecular barcoding, species delineation, Aculifera, Neomeniomorpha, worm-mollusc

INTRODUCTION

Two-thirds of the world's surface are constituted by the deep sea, providing one of the largest biomes of our planet (Danovaro et al., 2010). A plethora of different habitats and ecosystems such as plains, canyons, seamounts, hydrothermal vents, and cold seeps harbors an unknown magnitude of diversity, as large parts of the oceans' depths are still unexplored (Ramirez-Llodra et al., 2010). Efforts to increase knowledge on the deep sea—in terms of ecology, biodiversity and bathymetry—have triggered numerous expeditions to explore its inhabitants and ecosystems and consequently led to the discovery of hundreds of new species (e.g., Brandt et al., 2007). These discoveries emphasize the richness of yet unknown diversity in the deep sea and the need for basic α-taxonomic work to resolve what has been identified as the key shortfall of current biodiversity data. The lack of species taxonomy ("Linnean Shortfall" of biodiversity knowledge; Hortal et al., 2015), describing biodiversity at species level, affects and limits all approaches to understand distribution, abundance and evolutionary processes of deep-sea fauna.

Many paradigms in deep-sea research (e.g., on diversity gradients, bathymetric ranges, dispersal barriers, or the connectivity of populations) have been proposed based on a limited number of organisms linked to their specific biological traits and their general applicability still needs to be tested when broader data sets are available (see, e.g., Gage and Tyler, 1991; Rex et al., 2005, 2006; McClain and Hardy, 2010; Rex and Etter, 2010). In fact, recent studies have revealed taxon-specific patterns of bathymetric and geographic distribution, therein highlighting the potential pitfalls of generalizing single-taxon studies (McClain and Hardy, 2010). Comparative data from multiple taxonomic groups is needed to evaluate the role of specific biological traits and different evolutionary histories.

Frequently, available data on biodiversity is taxonomically biased toward larger, easily identifiable and well-known clades (Hortal et al., 2015) and with regard to molluscan deep-sea fauna research has largely focused on gastropods and bivalves (see, e.g., Rex, 1973; Bouchet and Warén, 1980; Zardus et al., 2006; Allen, 2008; Schrödl et al., 2011; Brault et al., 2013; Jörger et al., 2014). In faunistic analyses and biodiversity studies of benthic deep-sea communities the two classes of worm-molluscs are often lumped together in the generalizing supraclass term "Aplacophora" (see, e.g., Girard et al., 2016; Gutt et al., 2016; Román et al., 2016). The diversity within Caudofoveata (or Chaetodermomorpha) and Solenogastres (or Neomeniomorpha) is largely ignored, presenting a significant gap in detailed and comparative biodiversity information. To date, nearly 300 species of the small clade of Solenogastres are formally described, but estimates propose that its true diversity is at least 10-fold and many more novel species are routinely collected in the framework of e.g., biodiversity or monitoring surveys (Glaubrecht et al., 2005; Todt, 2013).

The lack of α-taxonomic work on Solenogastres is partially owed to their time-consuming and challenging taxonomic assignment, which requires studying a complex set of characters via various methods to reach suprageneric identification (Todt, 2013). Externally, Solenogastres can be differentiated based on aragonitic sclerites covering their entire body surface. This "scleritome" is unique to aplacophorans and in Solenogastres it consists of combinations of hollow or solid needles and scales of diverse shapes, arranged in single or several layers. Further important taxonomic characters are the radula and several anatomical and histological features of the digestive system (especially the foregut glands) and the gonopericardial system (Salvini-Plawen, 1978a,b; García-Álvarez and Salvini-Plawen, 2007). Identification to family level and beyond thus requires external investigations via light (LM) or scanning electron microscopy (SEM) and at least partial histological sectioning of the anterior and posterior part of the animal. The difficulty of solenogaster taxonomy is augmented by (1) the rarity of many lineages, (2) the small size of the majority of species, hampering the extraction of all necessary taxonomic characters from single individuals and (3) the reported co-occurrence of externally cryptic species (Bergmeier et al., 2016a). As a first step toward integrating solenogaster diversity in overall biodiversity assessments of deep-sea fauna we need an efficient and fast workflow able to reliably address species-level diversity collected in a certain region. This shall guarantee that the entire discovered diversity is initially characterized, providing the baseline for full taxonomic descriptions and further ecological or evolutionary approaches.

As in most marine invertebrates, solenogaster taxonomy and systematics show a strong geographical bias in biodiversity assessment because of historical collecting efforts. Due to the focus of taxonomic research on atlantic, mediterranean and antarctic Solenogastres almost two thirds of the known species diversity is described from these regions (see e.g., work by Salvini-Plawen, 1978a,b; García-Álvarez et al., 2014; Pedrouzo et al., 2014). In terms of their bathymetric distribution the majority of species has been described from the lower region of the continental shelf, around 22% (64 species) from bathyal depths and only 8% (18 species) are described from abyssal plains (extending between 4,000 and 6,000 m, as defined by Gage and Tyler, 1991). Currently, the majority of abyssal species belongs to the order Cavibelonia and is classified within five families, but two novel, undescribed species of the family Dondersiidae (order Pholidoskepia) have been recently reported from similar depths (Cobo et al., 2013). These species have all been described from either the Southern Atlantic (e.g., Gil-Mansilla et al., 2008) or Antarctica (Salvini-Plawen, 1978a,b). Only a single species has been collected below 4,000 m in the Pacific: *Pachymenia abyssorum* Heath, 1911 (Amphimeniidae) off the Californian coast (USA) in the beginning of the twentieth century.

The aim of the present study is to characterize the morphological and molecular diversity of abyssal Solenogastres, which were collected during the German-Russian joint "KuramBio (Kuril-Kamchatka Biodiversity Studies) Expedition" on board of R/V *Sonne* (SO 223) to the Northwest Pacific (NWP). The sampled abyssal Northwest Pacific Plain biogeographically belongs to the North Pacific Abyssal Province (Watling et al., 2013) and is situated in an eutrophic area of increased primary production, with uniform bathymetry and a mean depth of 5,000 m (Zenkevitch, 1963). To the west of the abyssal plain lies the Kuril-Kamchatka Trench, reaching down to 9,500 m.

The cold East Kamchatka Current, originating from the Bering Sea, influences especially the northern part of the trench and permeates into the semi-isolated Sea of Okhotsk (Qiu, 2001), which is connected to the open Northwest Pacific and its abyssal plain via two bathyal straits (Krusenstern and Bussol Strait). Following the routes of the Russian R/V *Vityaz* cruises from the mid twentieth century (Zenkevitch, 1963; Belyaev, 1983) the "KuramBio" expedition applied standardized deployments of state-of-the-art sampling gear to investigate 12 abyssal stations on the NWP Plain and close to the Kuril-Kamchatka Trench (see **Figure 1** for a station map of the expedition) (Brandt and Malyutina, 2012).

In summary, the present study has a two-fold focus: (1) develop an efficient workflow applicable also by non-specialists to initially characterize solenogaster diversity to make this neglected molluscan clade easier accessible to deep-sea research and (2) provide first insights into the still completely unknown abyssal solenogaster fauna from the NWP by using the proposed workflow. Despite being confronted with a sample dominated by singletons and hampered by incomplete datasets, we characterize the full diversity of abyssal Solenogastres collected during the KuramBio expedition. We identify three key lineages from the regionally most diverse families for further in depth taxonomic analyses and describe the novel abyssal species *Amboherpia abyssokurilensis* sp. nov. from the deep-sea family Acanthomeniidae based on 3D-microanatomical data.

MATERIALS AND METHODS

Sampling and Fixation

The KuramBio expedition on board of R/V *Sonne* set out to explore the benthos of the slope of the Kuril-Kamchatka Trench and the adjacent abyssal plain in the Northwest Pacific, east of the Kuril Island chain, at overall 12 stations (see **Figure 1**, **Table 1**). This study is based on the Solenogastres collected with a camera-equipped epibenthic sledge (C-EBS; Brandt et al., 2013) during this cruise. On deck, the complete C-EBS samples were transferred to pre-chilled (−20°C) 96% ethanol and stored in a −20°C freezer for at least 48 h for molecular analyses. Alternatively, 3.6% formalin-seawater was used as a fixative for some hauls. In the laboratories of R/V *Sonne* the samples were then identified and sorted on ice into metazoan phyla. At eight cruise stations (10 C-EBS hauls), from depths between 4,830 and 5,397 m, a total of 33 solenogaster specimens was collected. Thirty were fixed and stored in 96% ethanol and three (ZSM Mol20170086, −87, −88) fixed in 3.6% formalin-seawater. All specimens

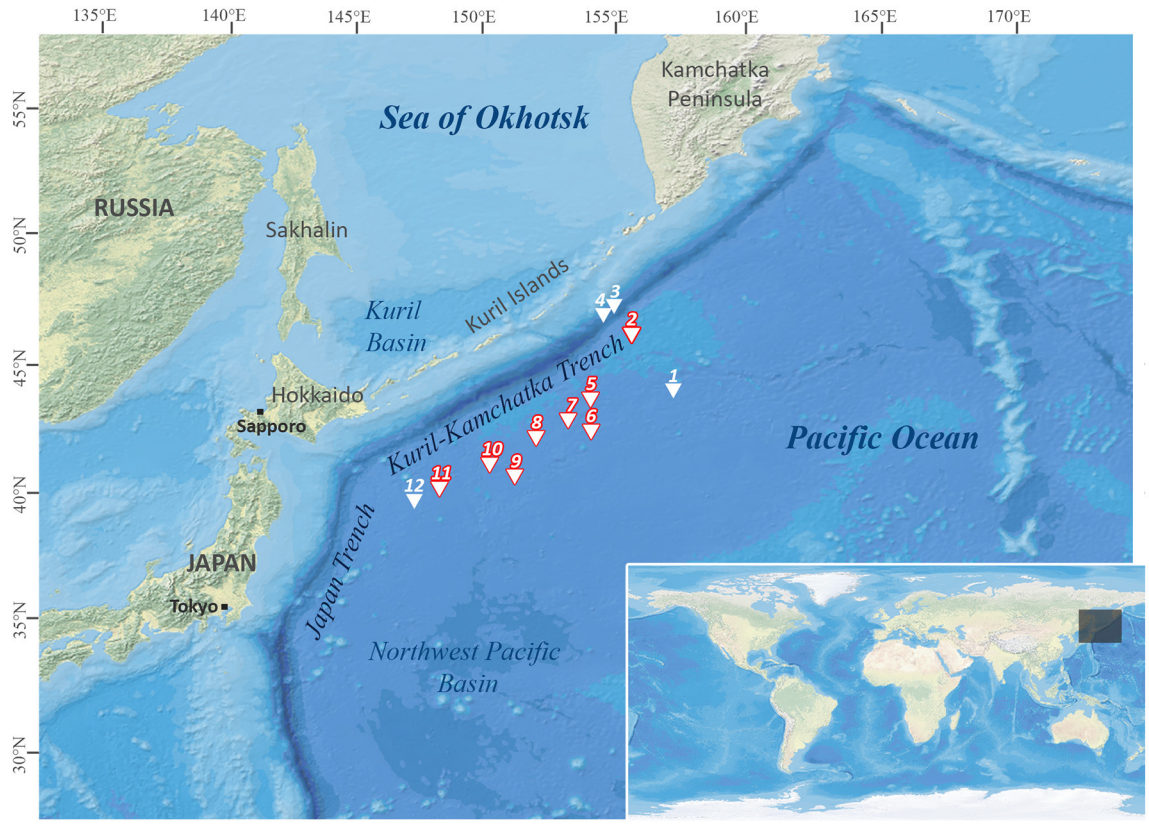

FIGURE 1 | Station map of the Kuril-Kamchatka-Biodiversity Studies (KuramBio) expedition. Stations emphasized in red: sampling sites where Solenogastres were collected. Map created with DivaGis.

TABLE 1 | Station table of the KuramBio expedition.

Station	Coordinates (Decimal Degree)	Depth (m)	Number of individuals
1	43.9710°N–43.9722°N; 157.3278°E–157.2995°E	5,412–5,429	0
2–09	46.2268°N–46.2487°N; 155.5567°E–155.5428°E	4,830–4,864	2
3	47.2307°N–47.2477°N; 154.6982°E–154.7197°E	4,859–4,863	0
4	46.9640°N–46.9747°N; 154.5398°E–154.5565°E	5,681–5,780	0
5–09	43.5913°N–43.5717°N; 153.9647°E–153.9693°E	5,376–5,379	3
6–12	42.4915°N–42.4704°N; 153.9989°E–153.9953°E	5,291–5,307	5
7–09	43.0437°N–43.0248°N; 152.9905°E–152.9727°E	5,216–5,223	3
7–10	43.0463°N–43.0276°N; 152.9882°E–152.9743°E	5,218–5,221	3
8–09	42.2447°N–42.2378°N; 151.7351°E–151.7082°E	5,125–5,140	4
8–12	42.2453°N–42.2387°N; 151.7391°E–151.7157°E	5,115–5,124	6
9–12	40.5918°N–40.5713°N; 150.9976°E–150.9864°E	5,392–5,397	5
10–12	41.1939 °N–41.2169°N; 150.0928°E–150.0942°E	5,249–5,262	1
11–12	40.2184°N–40.2018°N; 148.1088°E–148.0923°E	5,348–5,350	1
12	39.7300°N–39.70821°N; 147.18131°E–147.15621°E	5,215–5,228	0

Epibenthic sledge (C-EBS) sampling sites where Solenogastres were collected are highlighted in bold and also state the respective C-EBS haul number.

are deposited at the Bavarian State Collection of Zoology (ZSM) in Munich, Germany (see **Table 2** for overview of material).

Hard-Part Morphology via Light and Scanning Electron Microscopy

We took overview photographs of all specimens using a Leica camera mounted on a Leica Z16 APO compound microscope. Body length was measured after fixation in ethanol. Hard parts were analyzed via light (LM) and/or scanning electron microscopy (SEM) (see **Table 2**).

Specimen dehydration for SEM was achieved by slow, overnight evaporation of 100% dehydrated ethanol from glass vials containing the specimens. Each animal was mounted on a self-adhesive carbon sticker on a SEM-stub. We coated them with gold in Argon atmosphere for 240 s in a Polaron sputter coater (GaLaGabler Labor Instrumente Handels GmbH). SEM micrographs were taken with a LEO 1430 VP SEM (Zeiss). SEM specimens were then directly used for DNA extractions (see Bergmeier et al., 2016b). Specimens with sufficient body size (i.e., >2 mm) were divided using a razorblade. The posterior part was used for DNA extraction and the anterior part for manual preparation of the radula. Soft tissue was dissolved in a 3:1 solution of distilled water and household bleach and radula (if preparation was successful) and sclerites were documented via LM and SEM.

Histology and 3D-Reconstruction

One 3.6% formalin fixed specimen (ZSM Mol20170088) and two specimens fixed in 96% ethanol (ZSM Mol20170093 and 20170077) were selected for histological investigations. ZSM Mol20170077 was tri-sectioned. The midsection was used for DNA extraction (see below) and the anterior and posterior part processed for anatomical investigations: specimens were decalcified in 1% ascorbic acid over night, post-fixed with osmium tetroxide and embedded in Spurr's low viscosity resin (Spurr, 1969). Serial sections of 1 µm thickness were cut using a diamond knife on a RMC MT 7000 microtome (Leica AG). Contact cement on the lower cutting edge of the resin blocks ensured the formation of ribbons (Ruthensteiner, 2008). Ribbons were collected on microscopic slides, stained with azure II/methylene blue (Richardson et al., 1960) and sealed with cover slips. All sections were semi-automatically digitalized with a BX16VS Olympus microscope (20x magnification) in conjunction with the software DotSlide vs-ASW FL by Olympus. Digital files were exported as ".vsi" files and ".tif" images generated with the Olympus software OlyVia, using 16.5x magnification. All digital photos were converted to 8-bit grayscale, contrast enhanced and unsharp masked with Photoshop CS6 (Adobe Systems Software). The digitalized histological section series was imported into the 3D-vizualization software Amira 5.3.3 (Visage Imaging, FEI) and a computer based 3D-reconstruction of all major organ systems was carried out for specimen ZSM Mol20170088. Anatomy of specimens ZSM Mol20170093 and 20170077 was studied using Amira and schematic drawings were done with the freeware Inkscape (www.inkscape.org).

DNA Extraction, Barcode Amplification, and Sequencing

DNA extraction was done either by standard CTAB extraction, or by combining DNA extraction via CTAB with recovery of the DNA using spin-columns (Machery-Nagel Blood and Tissue Set). Dried and sputter-coated samples previously used for SEM investigations were ground up using pistils before tissue lyses (see Bergmeier et al., 2016b). We amplified mitochondrial 16S rRNA via PCR using the Phire II Hotstart polymerase (ThermoFischer) with the supplied 5x reaction buffer containing

TABLE 2 | Overview of all morphospecies of Solenogastres collected during the KuramBio cruise and the data generated from the respective individuals.

Species ID	ZSM Number Mol.	Station	Habitus	Approx. length (mm)	Scleritome			Radula	Barcode
					# Types of acicular sclerites	Types of scales	Foot scales		
Cavibelonia sp. 1	20170101	10–12	spiny	3	?	?	?	?	MG524989
Cavibelonia sp. 2	20170102	2–09	fuzzy	5	3○	1	b-s + bulge	?	MG524988
Cavibelonia sp. 3	20170103	6–12	furry	2.5	2○	?	?	?	?
Cavibelonia sp. 4	20170104	6–12	v. spiny	1	1○1●	3	b-s + bulge	?	?
Proneomeniidae sp. 1	20170100	8–09	v. smooth	3.5	1○	0	b-shape	?	MG524985
Halomeniinae sp. 1	20170076	5–09	fuzzy	2.5	2○	1	b-s + bulge	distichous	MG524986
	20170077*			1.7				distichous	MG524987
Pruvotinidae sp. 1	20170078	2–09	fuzzy	2	3○ + hooks	0	?	?	MG524984
	20170079	5–09	spiny	2	3○ + hooks	1	b-s	?	MG524982
Pruvotinidae sp. 2	20170080	7–09		2					MG524980
	20170081	7–10		2	3○ + hooks	1	b-s		MG524983
	20170082	8–09		2	3○ + hooks	1	b-s		MG524981
Pruvotinidae sp. 3	20170083	6–12	spiny	1.5	1○ + hooks	0	?	distichous	?
Simrothiellidae sp. 1	20170097	8–09	rough	1.2	3○	0	l-s	?	MG524979
Simrothiellidae sp. 2	20170098	8–09	rough	1.5	2○	1	?	?	?
Spiomenia sp.	20170099	6–12	v. spiny	2	3○	0	?	?	?
	20170089	7–10		3.5	4○	5	b-s + bulge	not present	MG524978
	20170090	7–10		3	4○	5	b-s + bulge	not present	MG524977
Veromenia cf. *singula*	20170091	8–12	fuzzy	2.2	4○	5	b-s + bulge	not present	MG524976
	20170092	8–12		2	4○	5	b-s + bulge	not present	MG524975
	20170093*	8–12		2.5				not present	
	20170084			3.5	3○	2	b-s + bulge		
Amboherpia abyssokurilensis sp. nov.	20170085			4.5	3○	2	b-s + bulge		
	20170086	9–12	smooth	5.5	3○	2	b-s + bulge	monoserial	?
	20170087			3	3○	2	b-s + bulge	monoserial	
	20170088* +			3.6				monoserial	
Acanthomeniidae sp. 1?	20170095	7–09	smooth to rough	2	2○2●	1	?	?	?
	20170096	8–12		2.5	2○2●	1			
Acanthomeniidae sp. 2	20170094	8–12	smooth	6.5	2○	5	b-s + bulge	?	?
Sterrofustia sp. 1	20170108	11–12	furry	2.7	2●	1	b-s	?	?
Dondersiidae sp. 1	20170106	6–12	velvety	3	1●	1	?	?	?
Dondersiidae sp. 2	20170107	8–12	smooth	3.5	2●	4	?	?	?
Dondersiidae sp. 3	20170105	7–09	spiny	1	1○1?	3	?	?	?

*White circle, hollow acicular elements. Black circle, solid acicular elements. ?, no data available for the entire clade, blanks indicate that this character set was not studied in the respective individual. *, histological section series available. +, holotype. b- or l-s, blade- or leaf-shaped; V., very.*

$MgCl_2$ as an additive. We used two different primer sets: 16S-S2 (Schwenk et al., 1998) and 16S-a (Simon et al., 1994) resulted in a sequence length of the amplified part of ∼470 base pairs. In addition, a pair of self-designed, solenogaster specific internal 16S rRNA primers (designed using Primer3; Untergasser et al., 2012) resulted in a sequence length of ∼360 base pairs: 16Soleno-r (5′-YYTAATCCAACATCGAGGTC-3′) and 16Soleno-f (5′-RRGAGTWAGRCCTGCCCAGT-3′). The following PCR specifics were used for amplification: 30 s at 98°C and (5 s at 98°C, 5 s at 47–50°C, 20 s at 72°C) × 35–37 and 60 s final elongation at 72°C. PCR products were cleaned up using the DNA Clean & Concentrator-5 (Zymo Research) and sent off for cycle sequencing (using Big Dye 3.1) on an ABI 3730 capillar sequencer at the Genomics Service Unit of the LMU Munich.

Molecular Sequence Data and Analyses

Overall we obtained 15 16S rRNA sequences. These were edited manually using the software Geneious 6.1 (Biomatters Ltd.) and a BLAST search against the existing databank was performed to check for any contaminated sequences. Sequences were aligned using the MUSCLE algorithm as implemented in Geneious, and ambiguous regions within the alignment were masked using GBlocks with options for less stringent selection (Castresana, 2000). We performed a maximum likelihood analysis using RAxML (Stamatakis, 2014) with the nucleotide substitution model GTR+G determined via jModelTest (Posada, 2008). In a pre-analysis we used a Caudofoveata 16S sequence from GenBank (AY340451) as outgroup to determine the basal lineage within our dataset. All sequence analyses were conducted using the CIPRES gateway (Miller et al., 2010).

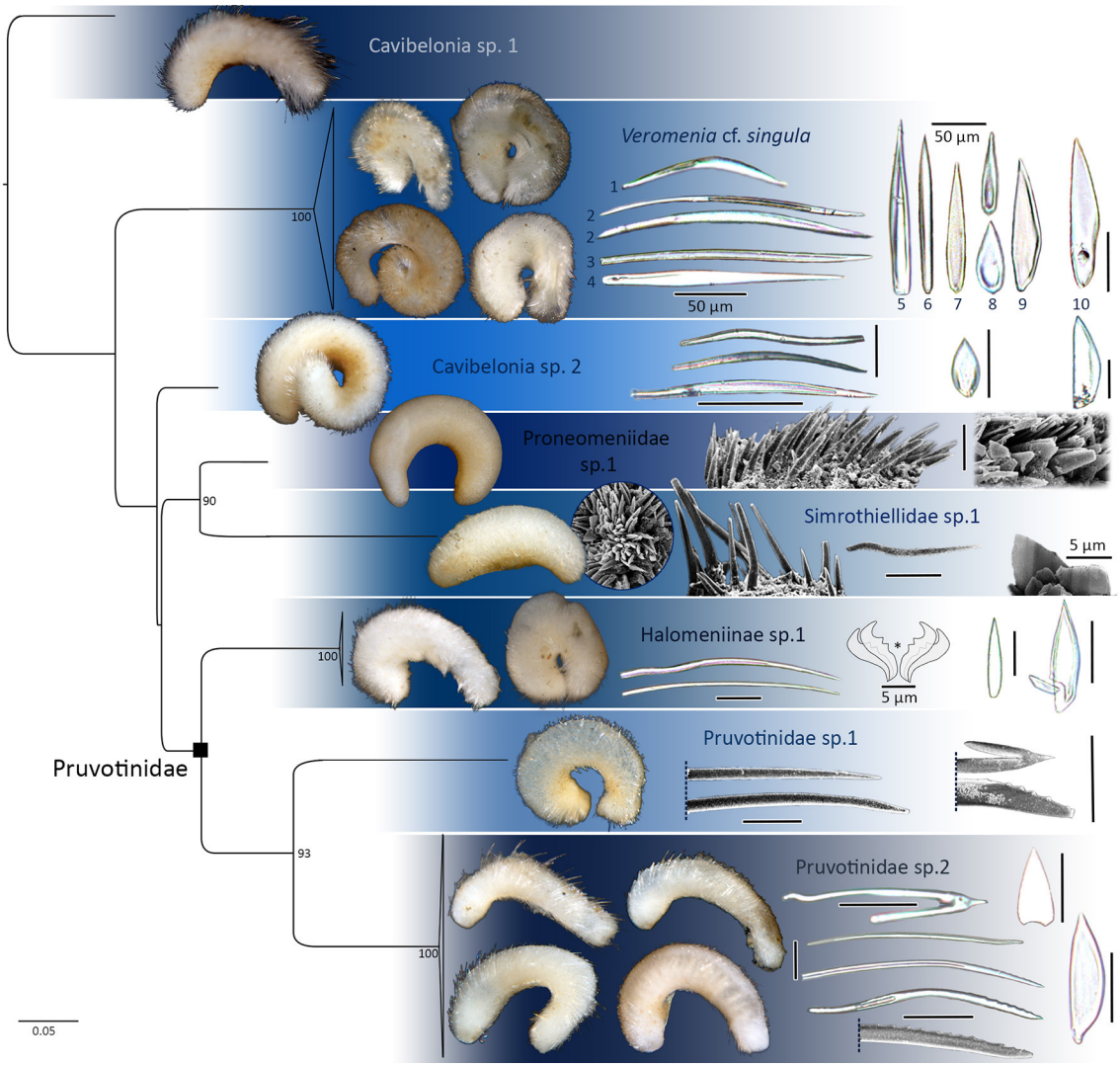

FIGURE 2 | 16S rRNA single gene maximum likelihood tree reconstructed with RAxML, bootstrap values of >85 plotted. Distinct lineages of Cavibelonia. Hard parts of respective lineages plotted. Asterisk in Halomeniinae sp. 1 marks radula. Foot scales always to the right. If not stated otherwise, all scleritome scale bars 25 µm.

For GenBank accession numbers of the generated barcodes see **Table 2**.

RESULTS

Diversity and Distribution

Based on molecular sequence data, morphology, and additional anatomical characters we were able to confidently differentiate 19 lineages of Solenogastres in our material, representing at least five different families. One potential additional lineage (referred to as Acanthomeniidae sp. 1?) cannot be delineated with certainty, due to lack of some important characters—see section Discussion. Of the 19 definite lineages present in our dataset eight are robustly supported by a combination of molecular and morphological data (see **Figure 2**). The delineation of the remaining 11 (or 12, including Acanthomeniidae sp. 1?) (morpho-) species is based on detailed hard-part features, i.e., scleritome and radula (**Figures 3–5**) and in three cases on additional anatomical data derived from histological serial sections (**Figures 6–10**). Identification to family level and beyond was possible for 11 species, respectively three species. We were not able to identify four lineages by comparing their scleritome with literature data of any of the currently existing families, and for now they remain identified to order level only. Cavibelonia sp. 1 (**Figure 2**) unfortunately lacks scanning electron or light microscopic scleritome data (see **Table 2**) since the specimen was lost during preparation.

With the exception of four individuals, all other collected specimens (29 individuals) belong to the order Cavibelonia. Within the cavibelonian lineages identified to family level and beyond, four families are represented by 12 species.

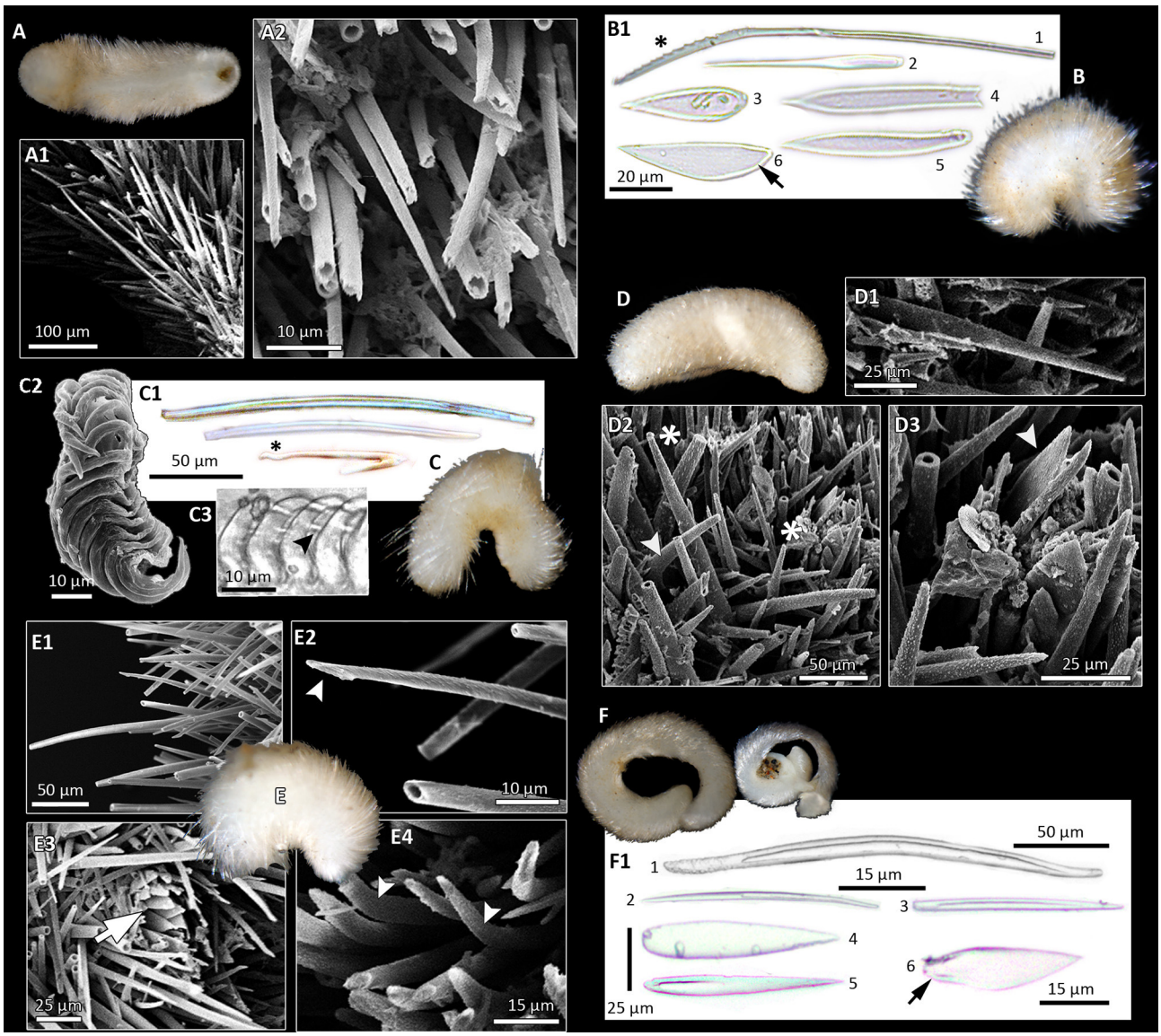

FIGURE 3 | Morphological diversity of Solenogastres, based on light (**B1,C1,C3,F1**; foot scales indicated by black arrows) and scanning electron microscopy of hard parts. Photographs of animals all taken after fixation in ethanol. **(A)** Cavibelonia sp. 3, covered in acicular, hollow needles **(A1)** of varying length, both straight and bent **(A2)**. **(B)** Cavibelonia sp. 4 with hollow and solid acicular elements and scales **(B1)**. Note proximal serrations (asterisk). **(C)** Pruvotinidae sp. 3 with acicular elements [straight and hook-shaped (asterisk)] **(C1)** and distichous radula (**C2,C3**—black arrowhead points to radula denticle). **(D)** Simrothiellidae sp. 2 with straight (**D1,D2** asterisk) and curved (**D2**, arrowhead) acicular hollow elements and scales (**D3**, arrowhead). **(E)** *Spiomenia* sp. with long acicular elements **(E1)** with captate distal ends (**E2**, arrowhead), scales surrounding the dorsoterminal sense organ (**E3**, arrow) and short, slightly curved elements (**E4**, arrowheads). **(F)** *Amboherpia abyssokurilensis* sp. nov. with **(F1)** hollow, acicular sclerites (top), and scales (bottom).

The non-cavibelonian individuals represent three morphospecies of the order Pholidoskepia and one of Sterrofustia. No lineages of the small order Neomeniamorpha were found.

Fifteen of the 19 distinct lineages were collected as singletons. With almost 40% of all collected individuals, Acanthomeniidae is the most common family, represented by at least three lineages found at Sts. 7, 8, and 9. Whereas less individuals of Pruvotinidae (eight specimens) were collected, representatives of the family occurred slightly more widespread at Sts. 2, 5, 6, 7, and 8 (see **Figure 1** and **Table 1**). Solenogastres were most abundant and diverse at St. 8, with overall 10 individuals belonging to seven species (excluding Acanthomeniidae sp. 1?), collected during two C-EBS hauls. At St. 7, six individuals were found and at Sts. 6 and 9 five individuals each. At St. 5 three individuals were found. At Sts. 10 and 11 only one singleton each was collected. We collected no Solenogastres from the two deepest stations (St. 3 and 4) from the slope of the Kuril-Kamchatka Trench.

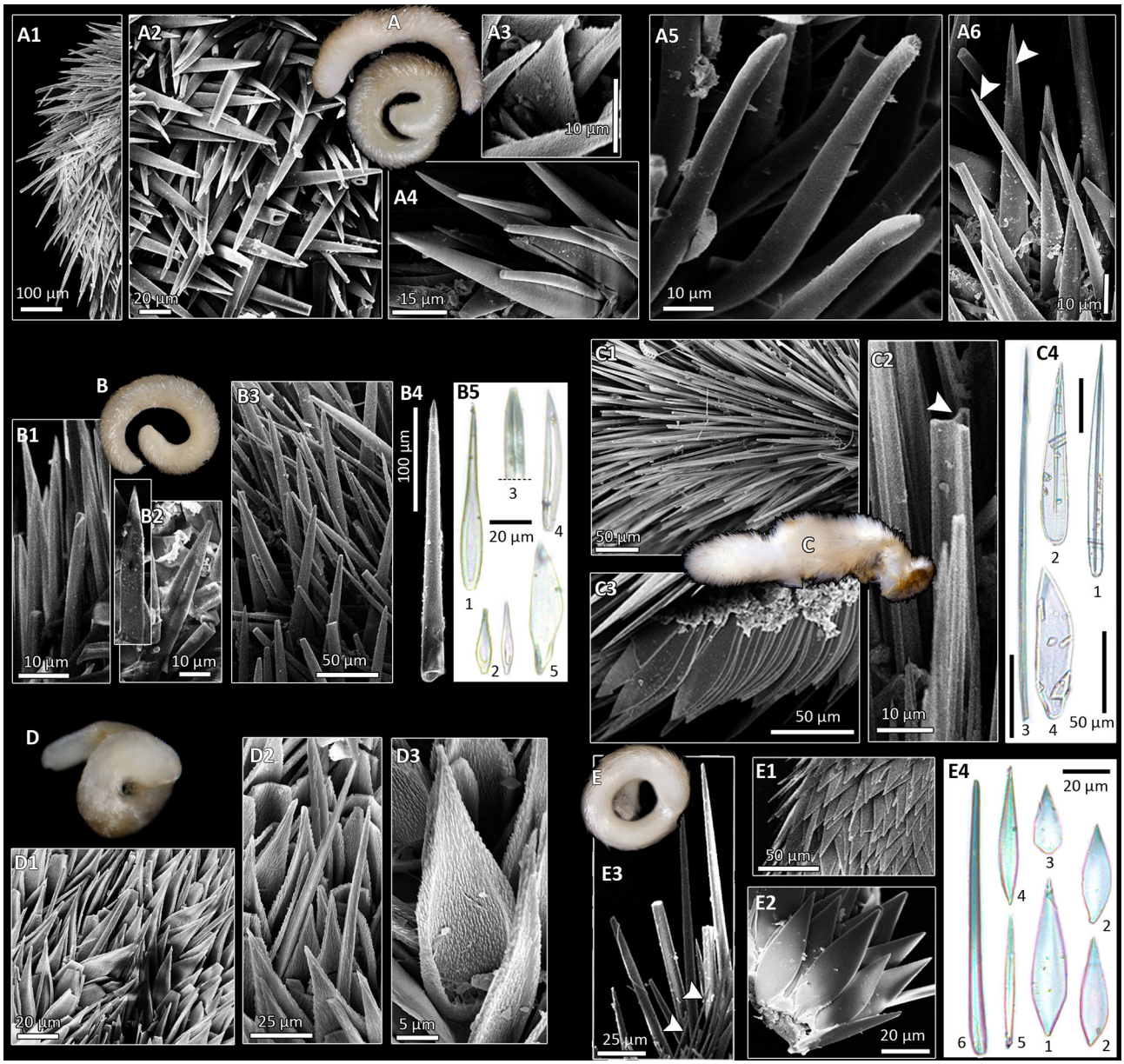

FIGURE 4 | Morphological diversity of Solenogastres, based on light **(B5,C4,E4)** and scanning electron microscopy of hard parts. **(A)** Acanthomeniidae sp. 1? **(A1)** Dorsal body with acicular spicules. **(A2)** Intercrossing hollow, needles. **(A3)** Leaf-shaped scale. **(A4)** Large and small needles. **(A5)** Sclerites with slight bend and distally thickened. **(A6)** Needles with distal keel (white arrowheads). **(B)** Acanthomeniidae sp. 1. **(B1)** Acicular, concave sclerite. **(B2)** Sclerites with thick lateral rims and flat back. **(B3)** Acicular sclerites of varying thickness and length *in situ* **(B3)** and one isolated **(B4)**. **(B5)** LM picture of different types of scales [foot scale (5)]. **(C)** Sterrofustia sp. 1 with a scleritome consisting of solid needles (**C1,C2** white arrowhead, **C4**) and blade-shaped foot scales [**C3,C4** (4)]. **(D)** Dondersiidae sp. 1 with a combination of needles and scales **(D1)**. **(D2)** Detail of short needles. **(D3)** Scale with rimmed base. Note hair-like ultrastructure of sclerite surfaces. **(E)** Dondersiidae sp. 2 covered with scales **(E1,E2)**. **(E3)** Long and thick as well as thin and short (white arrowheads) needles. **(E4)** LM images of sclerites.

Delimitation and Identification of Abyssal Solenogaster Lineages

The following species delimitation is based on external morphology of each lineage (remarks on coloration refer to the animal after fixation in ethanol), scleritome data (terminology mainly following García-Álvarez and Salvini-Plawen, 2007), radula (if radula extraction was successful) as well as genetic distances between sister clades in our one marker maximum likelihood analyses. For each lineage we differentiate between scales covering the body vs. scales surrounding the foot groove or dorsoterminal sense organ, since the latter two structures are always associated with scales. The term "sclerite" describes any element of the scleritome, whereas "spicule" refers to an elongated and needle-like structure in

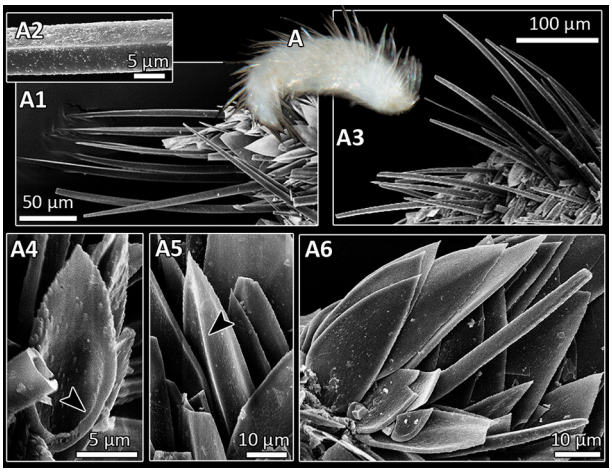

FIGURE 5 | Entire specimen **(A)** and SEM micrographs **(A1–A6)** of Dondersiidae sp. 3 **(A1)** Long spicules, straight and with keel **(A2)** or with slight bend **(A3). (A4)** Scale with rimmed base (arrowhead). **(A5)** Scale with median keel (arrowhead). **(A6)** Flat scale and short sclerite.

contrast to "scales". Foot scales are leaf- or blade-shaped, and the latter can be either of evenly convex shape [see, e.g., **Figure 2** (Pruvotinidae sp. 2)] or with a slight [**Figure 3B1** (6)] to distinct bulge (see, e.g., **Figure 2** *Veromenia* cf *singula*, Cavibelonia sp. 2).

See **Table 2** for a summary of all characters available for each clade and its individuals.

CAVIBELONIA Salvini-Plawen, 1978

Species belonging to this order in general exhibit a scleritome characterized by the presence of hollow, acicular needles ("spicules"). These can be combined with different types of scales, resulting in highly diverse scleritomes.

Cavibelonia sp. 1 (Figure 2):
Material: single specimen (ZSM Mol20170101).
Distribution: St. 10–12, 5,249–5,262 m.
Habitus: spiny, ∼3 mm in length; white coloration.
Scleritome: no scleritome data available, animal was lost during preparation.
Radula: unknown.
GenBank Accession Number: MG524989.
Interspecific genetic distance to sister clade based on 16S rRNA analyses: 23.1–37.0%.

Cavibelonia sp. 2 (Figure 2):
Material: single specimen (ZSM Mol20170102).
Distribution: St. 2–09, 4,830–4,864 m.
Habitus: fuzzy appearance, ∼5 mm in length; light yellow coloration.
Scleritome: dominated by three types of hollow, acicular sclerites of sigmoid shape, curved, and with broad mid-region. Leaf-shaped scales only. Foot scales blade-shaped with bulge.
Radula: unknown.

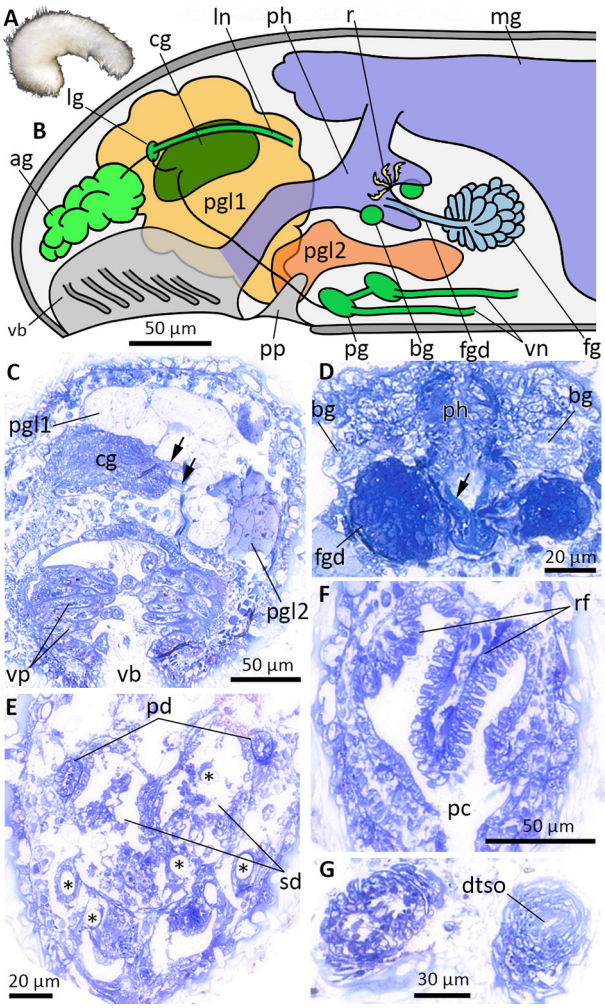

FIGURE 6 | Anatomy and histology of Halomeniinae sp. 1, highlighting the main taxonomic features. **(A)** Habitus. **(B)** Schematic illustration of the anterior body. **(C)** Cross-section at the level of the vestibular-buccal cavity. Arrows point to cerebrolateral (upper arrow) and cerebropedal (lower arrow) connectives. **(D)** Histology of the foregut gland ducts. Arrow points to radula tooth. **(E)** Cross-section through the posterior reproductive system at the transition of pericardioducts into paired spawning duct. Asterisks indicate hollows of dissolved body sclerites. **(F)** Respiratory folds in pallial cavity. **(G)** Section through the posteriormost part of the animal, before dorsoterminal sense organ (dtso) opens to the exterior. ag, accessory ganglia mass; bg, buccal ganglia; cg, cerebral ganglion; dtso, dorsoterminal sense organ; fg, ventrolateral foregut gland; fgd, duct of foregut gland; lg, lateral ganglion; ln, lateral nerve cord; mg, midgut; pc, pallial cavity; pd, pericardioduct; pg, pedal ganglion; pgl1/pgl2, type 1 and 2 of pedal glands; ph, pharynx; pp, pedal pit; rf, respiratory folds; sd, spawning duct; vb, vestibular-buccal cavity; vn, ventral nerve cord; vp, vestibular papillae.

GenBank Accession Number: MG524988.
Interspecific genetic distance to sister clade: 15.6–24.2%.

Cavibelonia sp. 3 (Figure 3A):
Material: single specimen (ZSM Mol20170103).
Distribution: St. 6–12, 5,291–5,307 m.
Habitus: furry appearance due to perpendicular projecting

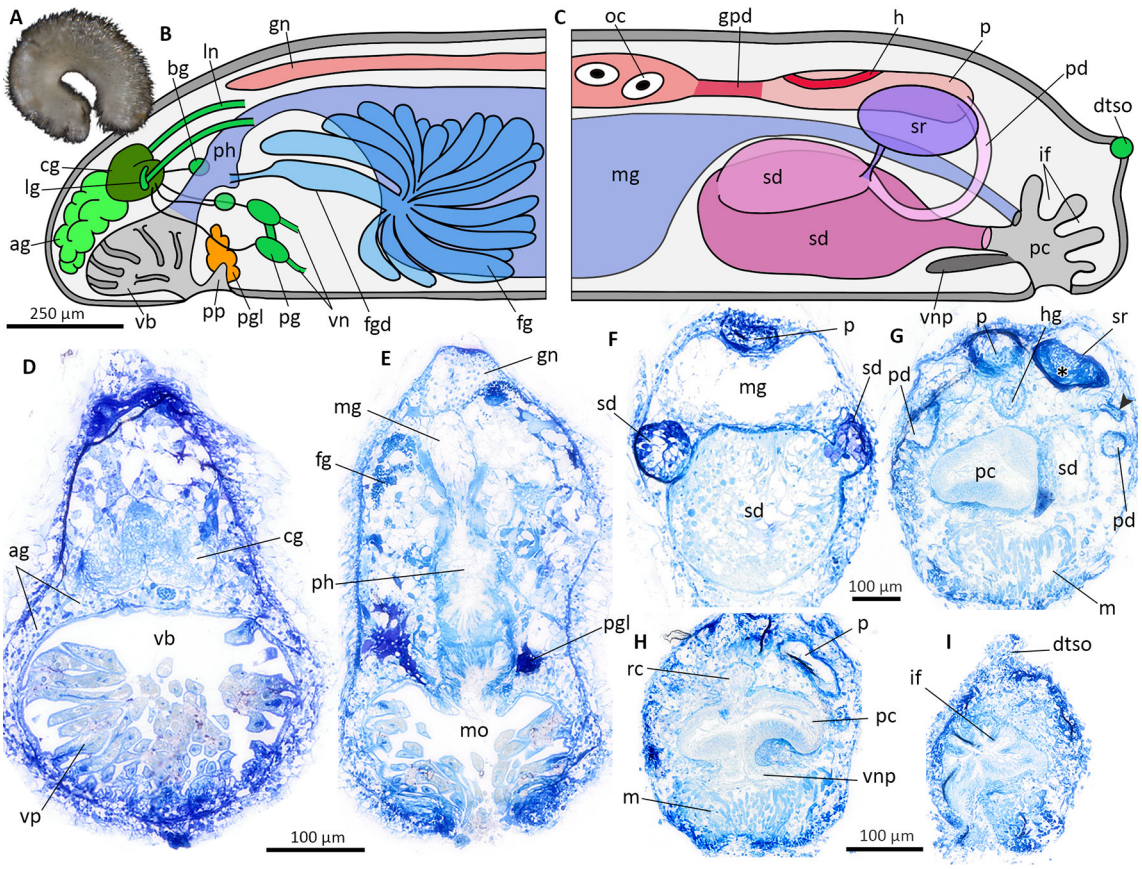

FIGURE 7 | *Veromenia* cf. *singula* **(A)** Habitus. Schematic illustration of the general anatomy **(B,C)**, histological cross sections **(D–I)**. **(B)** Anterior body. **(C)** Posterior body. **(D)** Vestibular-buccal cavity with cerebral ganglion and "accessory ganglia". **(E)** Anterior digestive tract with pharynx and midgut. **(F)** Reproductive system at the transition of pericardioducts and spawning duct. **(G)** Anterior part of pallial cavity and seminal receptacle filled with sperm (asterisk). Arrowhead points to duct connecting seminal receptacle and pericardioduct. **(H)** Pallial cavity with ventral pouch. **(I)** Dorsoterminal sense organ and epidermal infoldings of posterior pallial cavity. ag, accessory ganglia mass; bg, buccal ganglion; cg, cerebral ganglion; dtso, dorsoterminal sense organ; fg, ventrolateral foregut gland; fgd, duct of foregut gland; gn, gonad; gpd, gonopericardioduct; h, heart; hg, hindgut; if, epidermal infoldings; lg, lateral ganglion; ln, lateral nerve cord; m, muscle bundles; mg, midgut; mo, mouth opening; oc, oocyte; p, pericardium; pc, pallial cavity; pd, pericardioduct; pg, pedal ganglion; pgl, pedal gland; ph, pharynx; pp, pedal pit; rc, rectum; sd, spawning duct; sr, seminal receptacle; vb, vestibular-buccal cavity; vn, ventral nerve cord; vnp, ventral pouch; vp, vestibular papillae.

sclerites of equal length along the lateral sides (**Figures 3A,A1**), ∼2.5 mm in length; white coloration.
Scleritome: sclerites damaged, majority with broken tips. Two types of hollow, acicular elements discernible: one straight with pointed tip; second type with slight bend (**Figure 3A2**). No scales or foot scales observed.
Radula: unknown. No molecular data available.

Cavibelonia sp. 4 (Figure 3B):
Material: single specimen (ZSM Mol20170104).
Distribution: St. 6-12, 5,291–5,307 m.
Habitus: very spiny appearance, ∼1 mm in length; light yellow coloration.
Scleritome (**Figure 3B1**): two types of acicular elements: one hollow, distally bent with serrated end (**Figure 3B1**, asterisk) (200 µm length) (1), the other one solid with broadened proximal end (75 µm) (2). Three types of scales: leaf-shaped scales (50 µm) (3), groove-shaped sclerites with thickened lateral rims (up to 170 µm in length) (4) and slender elongated scales (60 µm in length) (5). Foot scales blade-shaped with bulge (50 µm length) (6).
Radula: unknown. No molecular data available.

Proneomeniidae Simroth, 1893
Representatives of this family are characterized by several layers of acicular sclerites of various shapes. Proneomeniidae sp. 1 was assigned to this family based on its very smooth appearance due to flatly arranged body sclerites, the slightly narrowed and flattened posterior end as well as the distinct yellow coloration after fixation in ethanol (see García-Álvarez et al., 1998).

Proneomeniidae sp. 1 (Figure 2):
Material: single specimen (ZSM Mol20170100).
Distribution: St. 8–09, 5,125–5,140 m.
Habitus: smooth appearance, ∼3.5 mm in length; body stout and thick, posterior tapering; strong yellow coloration.

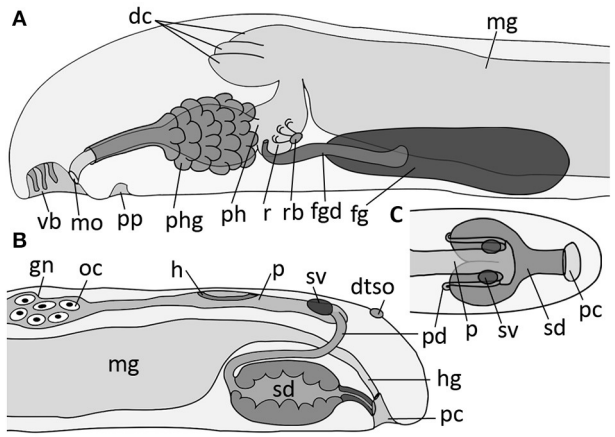

FIGURE 8 | Schematic illustration of main taxonomic characters of *Amboherpia abyssokurilensis* sp. nov. **(A)** Anterior digestive tract and **(B)** gonopericardial system, both in lateral view. **(C)** Posterior gonopericardial system, dorsal view. dc, dorsal caecum; dtso, dorsoterminal sense organ; fgd, duct of foregut gland; fg, ventrolateral foregut gland; gn, gonad; h, heart; hg, hindgut; mg, midgut; mo, mouth opening; oc, oocyte; p, pericardium; pc, pallial cavity; pd, pericardioduct; ph, pharynx; phg, pharyngeal gland; pp, pedal pit; r, radula; rb, radula bolster; sd, spawning duct; sv, seminal vesicle; vb, vestibular-buccal cavity.

Scleritome: specimen shrunk during drying process for SEM. Only one type of slightly curved hollow, acicular elements observed, projecting up to 40 μm from shrunken cuticle. Foot scales blade-shaped.
Radula: unknown.
GenBank Accession Number: MG524985.
Interspecific genetic distance to sister clade Simrothiellidae sp. 1: 26.7%.

Pruvotinidae Heath, 1911

The scleritome of Pruvotinidae is characterized by hollow acicular needles with occasionally serrated end, and the occurrence of hook-shaped elements in certain subfamilies.

With four species belonging to at least two subfamilies, Pruvotinidae is the most diverse family collected during the cruise. All of the pruvotinid species have hollow acicular elements in common, but vary in the presence of additional sclerites (e.g., hook-shaped elements are missing in the subfamily Halomeniinae - see below) and in the overall composition of their scleritome.

Halomeniinae sp. 1 (Figures 2, 6)

Material: two specimens (ZSM Mol20170076, 20170077).
Distribution: St. 5–09, 5,376–5,379 m.
Habitus: fuzzy appearance, ∼1.7 and 2.5 mm in length; white to light yellow coloration.
Scleritome: dominated by two types of hollow acicular elements, straight and with slight sigmoid shape (up to 120 μm long). One type of elongated scales, up to 75 μm in length. Foot scales blade-shaped (∼60 μm length).
Radula: distichous, each tooth (∼25 μm in length) with large lateral denticle and two smaller median denticles.
GenBank Accession Number: MG524986, −87.
Intraspecific genetic variability: 1.5%.
Interspecific genetic distance to sister clade Pruvotinidae sp. 1 and 2: 21.5–23.2%.

Anatomy of Halomeniinae sp. 1 *(Figure 6)*

Based on histological serial sections of ZSM Mol20170077 (**Figure 6A**, fixed specimen). Vestibular-buccal cavity common, with numerous papillae (**Figures 6B,C**), followed by conspicuous pedal pit with two types of pedal glands (**Figure 6B**). Pedal gland 1 large and extending far into head region, no particular staining properties. Pedal gland 2 smaller and extending posterior, staining light-purple (**Figure 6C**). Cerebral ganglion with two laterally emerging connectives leading to paired lateral and pedal ganglia (**Figures 6B,C**). From lateral ganglion, nerve exits toward "accessory ganglia" (i.e., pre-cerebral ganglia) dorsal to vestibulum; posterior the lateral nerve cords emerge on each side. Paired pedal ganglia with commissure; ganglia giving rise to ventral nerve cords. Small paired buccal ganglia present on both sides of radula (**Figure 6D**). Dorsoterminal sense organ present (**Figure 6G**). Mouth opening located in posterior part of vestibular-buccal cavity. Pharynx ciliated, with distichous radula (**Figures 2**, **6D** arrow). Foregut glands comprised of ducts with surrounding muscle layer (**Figure 6D**), posterior surrounded by gland cells (Type *Pararrhopalia* = Type A). Midgut with dorsal caecum, cnidocysts in midgut indicate cnidarivory of species. Hindgut opens into dorsoanterior part of pallial cavity. Gonads not present on section series of posterior third of body - either not developed due to immaturity or lost during tri-partitioning of specimen for DNA extraction. Paired pericardioducts opening into paired spawning duct (**Figure 6E**). Spawning duct fuses, but transition into pallial cavity (secondary genital opening) not detectable. Large hollows of dissolved spicules in ventroposterior part of animal most likely from copulatory spicules. Additional hollows indicate that body spicules reach from dorsal part inside of the animal to the ventral side and exit through cuticle (**Figure 6E**, asterisks). Pallial cavity with three respiratory folds (**Figure 6F**).

Taxonomic remarks

The posterior body, especially the entire reproductive system, could not be unambiguously reconstructed due to poorly preserved and for some parts destroyed histology. The combination of hard-part and anatomical features (no hook-shaped sclerites, foregut glands of Type *Pararrhopalia*, lack of pharyngeal glands, presence of respiratory folds) suggest the placement of this lineage within the subfamily of Halomeniinae. The single genus *Halomenia* Heath, 1911 is characterized by separated vestibulum (=atrium) and mouth opening, unpaired secondary genital openings (=unpaired opening of the spawning duct into the pallial cavity), the lack of copulatory spicules and the presence of a dorsoterminal sense organ and respiratory folds. Whereas the latter two features are present in our lineage, vestibulum and mouth opening share a common cavity (vestibular-buccal cavity) and copulatory spicules are present, but the state of the secondary genital opening cannot be

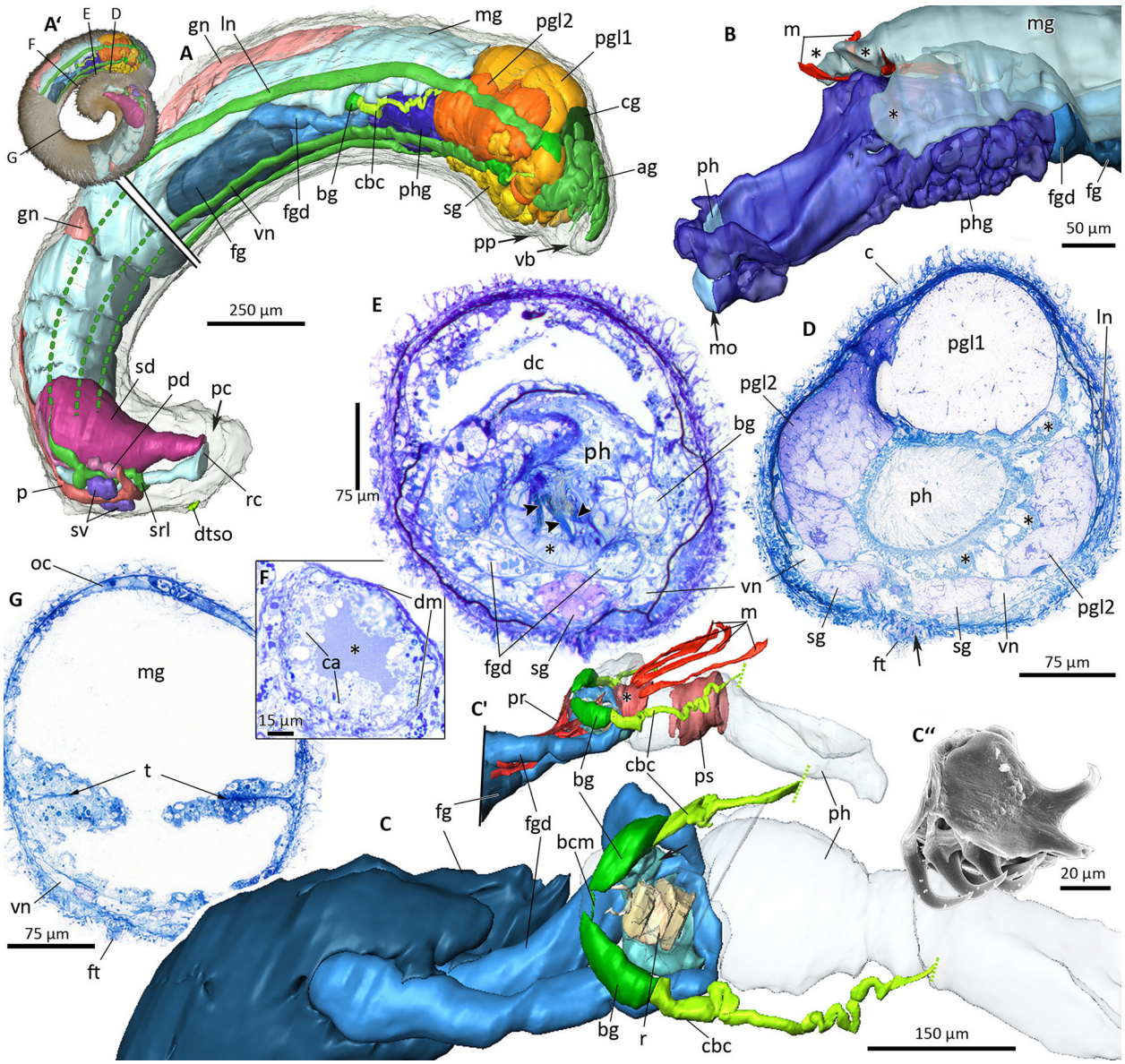

FIGURE 9 | 3D-microanatomy of *Amboherpia abyssokurilensis* sp. nov. **(A–C′)** with histological details of the digestive tract **(D–G)**. **(A′)** Habitus prior to sectioning, showing the regions that were used for the 3D-reconstructions. Black labeled lines indicate levels of respective histological sections. **(A)** 3D-reconstruction of all major organ systems, lateral view. Lateral and ventral nerve cords only partially reconstructed in the posterior half, as indicated by dotted lines. **(B)** Pharynx with surrounding pharyngeal glands and tripartite midgut caecum (asterisks), anterolateral view. **(C)** Anterior digestive tract showing the position of the radula within the pharynx (pharynx transparent, midgut, and pharyngeal glands omitted), dorsolateral view. **(C′)** Pre-radula sphincter (asterisk) and muscle fibers associated with the structures of the anterior alimentary tract, lateral view. **(C″)** SEM micrograph of radula, orientation as in living animal. **(D)** Histology of pharynx and pharyngeal glands (asterisks), pedal gland type 1 and 2. Arrow points to opening of sole glands. **(E)** Digestive tract at the level of radula (arrowheads) and radula bolster (asterisk). **(F)** Detail of the foregut gland duct with its lumen (asterisk), apices of gland cells and surrounding muscle layer. **(G)** Midregion of the body, showing typhlosolis formed by infoldings of the gut epithelium. ag, accessory ganglia mass; bcm, buccal commissure; bg, buccal ganglion; c, cuticle; ca, apical part of gland cells; cbc, cerebrobuccal connective; cg, cerebral ganglion; dc, dorsal caecum; dm, muscle layer surrounding duct; dtso, dorsoterminal sense organ; fg, ventrolateral foregut gland; fgd, ducts of foregut glands; ft, foot; gn, gonad; ln, lateral nerve cord; m, dorsopharyngeal muscle; mg, midgut; mo, mouth opening; oc, oocyte; p, pericardium; pc, pallial cavity; pd, pericardioduct; pgl1, pedal gland type 1; pgl2, pedal gland type 2; ph, pharynx; phg, pharyngeal gland; pp, pedal pit; pr, pharynx retractor muscle; ps, pharyngeal muscle sheath; r, radula; rc, rectum; sd, spawning duct; sg, sole gland; srl, suprarectal loop; sv, seminal vesicle; t, typhlosolis; vb, vestibular-buccal cavity; vn, ventral nerve cord.

ascertained from our material. Due to the problematic fixation and preservation of the material for histological purposes and the lack of complete information on the reproductive system, we refrain from establishing a novel genus within Halomeniinae. We postpone the formal description of this species, with the possibility of linking individuals collected in the

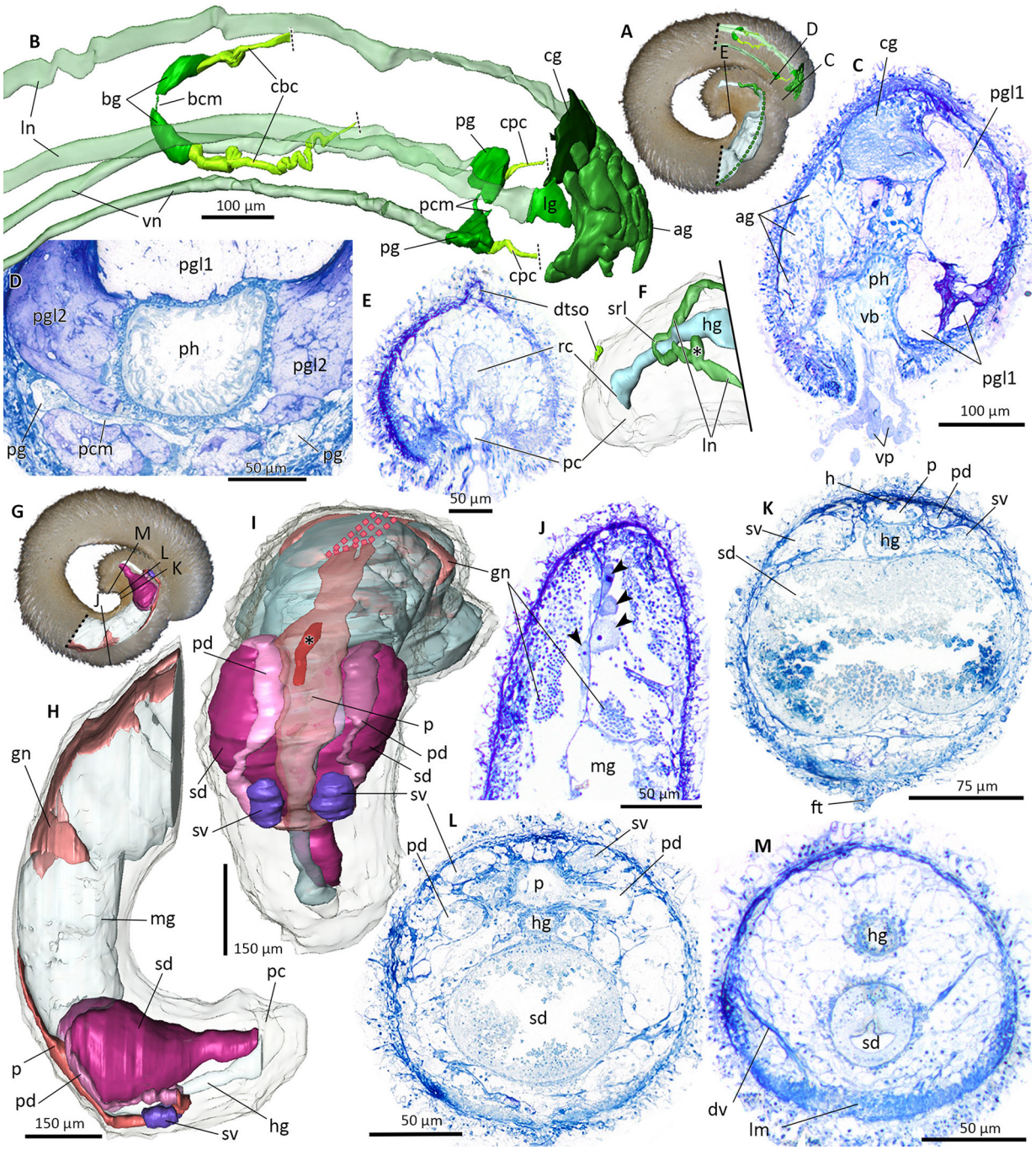

FIGURE 10 | Nervous system **(A–F)** and reproductive system **(G–M)** of *Amboherpia abyssokurilensis* sp. nov. in 3D **(A,B,F,H,I**–dotted lines indicate areas which could not be reconstructed) and histology from cross-sections **(C–E, J–M)**. **(A)** Position of reconstructed nervous structures within animal. Black labeled lines indicate level of histological sections. **(B)** Anterior nervous system. Lateral and ventral nerve cords transparent. Dorsolateral view. **(C)** Atrium at the transition into the pharynx. **(D)** Pedal ganglia and pedal commissure. **(E)** Dorsoterminal sense organ. **(F)** Posterior nervous system, body transparent. Dorsolateral view. Asterisk marks ganglia-like swelling of lateral nerve cord. **(G)** Position of reconstructed reproductive organs within animal, black labeled lines indicate levels of respective histological sections. **(H)** Lateral view of the reproductive system. Gut and body transparent. **(I)** Dorsal view of the reproductive system. Pericardium (transparent) with heart (asterisk). **(J)** Histology of the gonad, showing oocytes (arrow heads) along the median septum and spermatocytes. **(K)** Anterior part of the spawning duct, still bilobed, filled with secretion. **(L)** Fused mid part of spawning duct. **(M)** Posterior part of the spawning duct. ag, accessory ganglia mass; bcm, buccal commissure; bg, buccal ganglion; cbc, cerebrobuccal connective; cg, cerebral ganglion; cpc, cerebropedal connective; dtso, dorsoterminal sense organ; dv, dorsoventral musculature; ft, foot; gn, gonad; h, heart; hg, hindgut; lg, lateral ganglion; lm, longitudinal musculature; ln, lateral nerve cord; mg, midgut; p, pericardium; pc, pallial cavity; pcm, pedal commissure; pd, pericardioduct; pg, pedal ganglia; pgl1, pedal gland type 1; pgl2, pedal gland type 2; ph, pharynx; rc, rectum; sd, spawning duct; srl, suprarectal loop; sv, seminal vesicle; vb, vestibular-buccal opening; vn, ventral nerve cord; vp, vestibular papillae.

future with this lineage via the provided barcode and hopefully delivering all necessary features for a detailed integrative species description.

Pruvotinidae sp. 1 (Figure 2):
Material: single specimen (ZSM Mol20170078).
Distribution: St. 2–09, 4,830–4,863 m.
Habitus: fuzzy appearance, ∼2 mm in length, light yellow coloration with thin and transparent cuticle.
Scleritome: dominated by three types of hollow acicular spicules, straight with either pointed or serrated ends and one type curved (both up to 200 μm). Interspersed hook-shaped elements with pointed curvature, present along the dorsal side of the body. No further sclerites discernible due to shrinkage of animal during SEM preparation.
Radula: unknown.
GenBank Accession Number: MG524984.
Interspecific genetic distance to sister clade Pruvotinidae sp. 2: 21.5–23.9%.

Pruvotinidae sp. 2 (Figure 2):
Material: four specimens (ZSM Mol20170079, −80, −81, −82).
Distribution: Sts. 5–09, 8–09, 7–09, 7–10, 5,125–5,379 m.
Habitus: spiny appearance with several sclerites conspicuously longer than rest of scleritome; ∼2 mm in length, head region slightly enlarged in comparison to rest of body; white coloration.
Scleritome: dominated by three types of hollow, acicular sclerites: slightly curved with either pointed or serrated distal end (up to 400 μm) or of sigmoid shape with serrated distal ends (190 μm). Hook-shaped elements present with curve at proximal base, pointed at distal curvature (length 50 μm). One type of triangular scales (35 μm length). Foot scales: blade-shaped (45 μm).
Radula: unknown.
GenBank Accession Number: MG524980, −81, −82, −83.
Intraspecific variation: 0.4–1.0%.
Interspecific genetic distance to sister clade Pruvotinidae sp. 1: 21.5–23.9%.

Pruvotinidae sp. 3 (Figure 3C)
Material: single specimen (ZSM Mol20170083).
Distribution: St. 6–12, 5,291–5,307 m.
Habitus: spiny, several sclerites conspicuously larger than rest of scleritome (**Figure 3C**); ∼1.5 mm in length; white to light yellow coloration.
Scleritome: dominated by one type of hollow, acicular sclerites curved with slight bend, no serrated distal end (up to 250 μm length). Hook-shaped elements present, curved at proximal base, pointed at distal curvature (length 75 μm) (**Figure 3C1**). Type of foot scales unknown.
Radula: distichous, each tooth with one large lateral denticle and at least two smaller median denticles (**Figures 3C2,C3**). No molecular data available.

Simrothiellidae Salvini-Plawen, 1978
The scleritomes within this family are highly variable and can reach from hollow or solid acicular needles to more scaly sclerites arranged in up to several layers. We identified three different simrothiellid species, all collected as singletons. Habitus and scleritome of Simrothiellidae sp. 1 and sp. 2 are highly similar, but the two species differ in the presence (sp. 1) respectively absence (sp. 2) of a dorsoterminal sense organ (DTSO), observed using SEM. Due to the presence of captate sclerites and a dorsoterminal sense organ, the identification of the third lineage to genus level (*Spiomenia* sp.) is possible without additional anatomical characters.

Simrothiellidae sp. 1 (Figure 2):
Material: single specimen (ZSM Mol20170097).
Distribution: St. 8–09, 5,125–5,140 m.
Habitus: rough appearance, ∼1.2 mm in length, stout body; yellow coloration.
Scleritome: dominated by three types of hollow, acicular elements: straight with pointed distal end, one curved, one of sigmoid-shape (about 60 μm in length). Leaf-shaped scales visible surrounding a dorsoterminal sense organ. Foot scales leaf-shaped.
Taxonomic remarks: curved and sigmoid hollow spicules similar to the spicules of this species have been described for e.g., *Simrothiella comorensis* (see Figure 4A in Todt and Salvini-Plawen, 2003).
However, Simrothiellidae sp. 1 additionally has straight spicules which are lacking in *S. comorensis*.
Radula: unknown.
GenBank Accession Number: MG524979.
Interspecific genetic distance to sister clade Proneomeniidae sp. 1: 26.7%.

Simrothiellidae sp. 2 (Figure 3D):
Material: single specimen (ZSM Mol20170098).
Distribution: St. 8–09, 5,125–5,140 m.
Habitus: rough appearance, ∼1.5 mm in length, stout body; yellow coloration.
Scleritome: two types of hollow, acicular sclerites (up to 100 μm): straight with pointed distal end (**Figures 3D1,D2** asterisks) and curved sclerites (**Figure 3D2,** white arrowhead). No dorsoterminal sense organ. Elongated leaf-shaped scales of one type only (**Figure 3D3**, white arrowhead). No information on foot scales.
Radula: unknown. No molecular data available.

Spiomenia sp. (Figure 3E):
Material: single specimen (ZSM Mol20170099).
Distribution: St. 6–12; 5,291–5,307 m.
Habitus: very spiny appearance, stout body, 2 mm length; white coloration.
Scleritome: dominated by three types of hollow acicular sclerites, majority with pointed distal ends (**Figure 3E1**) or captate (distal end asymmetrically enlarged, **Figure 3E2**, white arrowhead), others with curved distal portion (**Figure 3E4**, white arrow head). Scales surrounding dorsoterminal sense organ only (**Figure 3E3**, white arrow). No information on foot scales. Radula: unknown. No molecular data available.

Acanthomeniidae Salvini-Plawen, 1978
Solenogastres with thin cuticle, hollow acicular sclerites and scales. Radula either monoserial or absent. Ventrolateral foregut glands of Type *Acanthomenia* (Type A sensu Salvini-Plawen, 1978a; Gil-Mansilla et al., 2008).

Veromenia *cf.* singula *(Figures 2, 7):*
Material: five specimens (ZSM Mol20170089, −90, −91, −92, −93).
Distribution: Sts. 7–10 and 8–12, 5,115–5,221 m.
Habitus: fuzzy appearance, ∼2–3.5 mm in length; coloration ranging from white to light orange (**Figure 2**).
Scleritome (**Figure 2** *Veromenia* cf. *singula* 1-10): dominated by four types of hollow, acicular elements: short and strongly curved (250 μm) (1), slightly curved, with varying thickness (2), straight (3), straight with widened mid-region and pointed distal end (4); (2)–(4) all up to 300 μm in length. Five types of scales: with folded lateral edges (5), rod-shaped with pointed distal end (6) rimmed and elongated (7), rimmed and leaf-shaped of varying length (8), blade-shaped with rim (9). Foot scales (10): blade-shaped with rimmed base and bulge. Without radula.
GenBank Accession Number: MG524975, −76, −77, −78.
Intraspecific genetic variability: 1.6–3.8%.
Interspecific genetic distance to sister clade: 21.4–33.4%.

Anatomy of Veromenia cf. singula
The anatomy of *Veromenia* cf. *singula* is based on histological serial sections of ZSM Mol 20170093 (**Figure 7A**, animal after fixation in ethanol). Vestibular-buccal cavity with papillae (**Figures 7B,D**); pedal pit small, with one type of pedal gland (**Figures 7B,E**). Cerebral ganglion fused with four nerve cords along lateral and ventral body wall (**Figures 7B,D**). "Accessory ganglia" mass (=pre-cerebral ganglia), paired buccal ganglia, and paired pedal ganglia present (**Figure 7B,D**). Dorsoterminal sense organ located dorsoposterior to pallial cavity (**Figures 7C,I**). Mouth opening located in dorsoposterior region of vestibular-buccal cavity. No radula present, pharynx leads directly into midgut (**Figure 7E**); no dorsal midgut caecum, no lateral constrictions. Hindgut opens dorsal into pallial cavity (**Figures 7C,H**). Ventrolateral foregut glands of Type *Acanthomenia* (**Figures 7B,E**) (definition according to Handl and Todt, 2005). Gonad extending far anterior (**Figures 7B,E**). Connected to pericardium via gonopericardioducts; paired ciliated pericardioducts leading into paired spawning ducts (**Figures 7C,F**). Seminal receptacle with sperm connected to dorsoanterior part of spawning duct (**Figures 7C,G**). Pallial cavity with infoldings (**Figures 7C,I**), but no true respiratory folds (compare **Figure 6F** for respiratory folds); ventral pouch connected to anterior part of pallial cavity (**Figures 7C,H**) with underlying conspicuous muscle layer (**Figures 7G,H**).

Taxonomic remarks
Anatomy and histology of the encountered lineage hardly differ from the holotype of the species (Gil-Mansilla et al., 2008), but the scleritome of the present material is more diverse than shown in the original species description (**Figure 2** sclerites 1, 3, 4, 6, 7, 9 not depicted in original description). Since intraspecific variation of scleritomes and distribution ranges in Solenogastres are still largely unknown, our species assignment is still tentative.

Amboherpia abyssokurilensis *sp. nov. (Figures 3F, 8–10)*
Material examined: Holotype (ZSM Mol20170088, histological section series), paratypes1-4 (ZSM Mol20179984-87) used for examination of the scleritome and preparation of the radula (ZSM Mol20170086, radula SEM mounted).
ZooBank registration: urn:lsid:zoobank.org:pub:A85AFE00-14C8-469D-A797-594C7DB3DB7A.
Type locality: Northwest Pacific, near Kuril-Kamchatka Trench, KuramBio Station 9-12 (40.5918°N–40.5713°N; 150.9976°E–150.9864°E), 5,392–5,397 m depth.
Etymology: Referring to the type locality of the species on the abyssal plain close to the Kuril-Kamchatka Trench.
Diagnosis: Hollow, acicular sclerites and two different types of solid body scales. Pharynx with pharyngeal glands, midgut without constrictions, but lateral typhlosolis. Radula teeth up to 50 μm at widest part of base. No esophagus. No sphincter muscle surrounding secondary genital opening (=opening of spawning duct).

Description
Smooth appearance; body round in diameter, ∼3.6 mm in length. Body white in fixed condition (**Figures 3F**, **9A′**). Cuticle up to 25 μm thick, no epidermal papillae. Scleritome (**Figure 3F1**): three types of hollow, acicular elements; most common one curved with flattened distal end (250 μm length) (1); slightly curved (ca. 50 μm) (2) and straight (40 μm) (3). Two types of body scales: flat (3) and with rim at proximal base (4). Foot scales blade-shaped with slight bulge (5). Vestibulum (=atrium) and buccal opening fused into single vestibular-buccal cavity (**Figure 8A**), with at least three discernible, unbranched vestibular papillae protruding from dorsoanterior wall. Foot emerges posterior to vestibular-buccal opening from inconspicuous pedal pit and terminates anterior to small pallial cavity. Two types of pedal glands open into the pedal pit. Type 1 fills most of the head region (**Figures 9A,D**), and stains whitish to very light pink. Type 2 is smaller, present on both sides of pedal pit and stains in a slightly darker pink compared to Type 1 (**Figure 9D**). Both of diffuse appearance, but clearly delimited by thin layer of connective tissue. Both discharge secretions directly into pedal pit. Sole glands as unicellular glands distributed evenly along both sides of foot groove (**Figure 9A**, shown only in the anterior part of the reconstruction). Light-purple staining secretions are discharged by each cell via minute outlets along the foot (**Figure 9D**, arrow).

Digestive system
The digestive system consists of pharynx, midgut, and the associated glands (**Figures 8A**, **9**). Mouth opening located in dorsoposterior region of vestibular-buccal opening (**Figures 8A**, **9A**). Pharynx (up to level of radula) surrounded by unicellular pharyngeal glands, each discharging light-purple staining secretions into pharyngeal lumen (**Figures 9B,D** asterisks). Pharynx divided into two histologically distinct parts: first part ciliated (**Figure 9D**), after pharyngeal sphincter

(**Figure 9C′**) lined with pseudostratified, glandular epithelium. After pharyngeal muscle sheath (**Figure 9C′**, asterisk), pharynx contains radula, which rests on several muscular radula bolsters (as defined by Handl and Salvini-Plawen, 2002) (**Figure 9E,** asterisk). Radula monoserial: five rows of teeth (**Figures 9C,C′′,E**) discernible in serial section (only three shown in reconstruction); base of tooth almost 50 μm wide, two hook-shaped hollow denticles (∼45 μm long) bend dorsal from each tooth (**Figure 9C′′**). Paired ventrolateral foregut glands of Type *Acanthomenia* (Handl and Todt, 2005) open into pharynx on each side laterally to radula (**Figures 8A**, **9C**). Each duct ∼300 μm long, comprising supporting cells and cell necks of glandular cells (cell apices) surrounded by muscular sheath (**Figure 9F**). Ducts posterior surrounded by large mass of somata of glandular cells, which produce dark-purple staining secretions. Secretions released into duct lumen via cell apices (**Figure 9F**). Pharynx connected almost vertically with midgut (**Figure 8A**); anterior midgut ceacum present, divided into three parts by muscles connecting pre-radula sphincter with dorsal body wall [**Figures 8A**, **9B,C′** (asterisks)]. In the mid region of animal, lateral walls of midgut epithelium form a typhlosole-like horizontal fold (**Figure 9G**). Midgut narrows into ciliated hindgut, opening into dorsoanterior region of pallial cavity.

Nervous system and sensory structures

Anterior central nervous system consists of cerebral ganglion, mass of pre-cerebral "accessory ganglia," paired buccal and pedal ganglia and four nerve cords (**Figures 10A,B**). Cerebral ganglion without median sulcus, at least two anterior cerebral nerves connect it to "accessory ganglia" mass; this mass is an interconnected accumulation of spherical bodies presumably comprised of neural tissue; clearly delimited by connective tissue and with random distribution of neuropil and perikarya (**Figure 10C**). At least four nerves run from accessory ganglia toward vestibulum. A short cerebrolateral connective emerges posteriorlaterally from each side of cerebral ganglion. Lateral nerve cords emerge from lateral ganglia and extend along lateral body wall toward posterior end of the animal (**Figure 10A**). Single nerve from left lateral ganglion innervates vestibular papillae. Paired buccal ganglia located dorsoposterior to radula, interconnected via thin and short buccal commissure (**Figures 9C**, **10A**).

Origin of cerebropedal and -buccal connectives not identifiable on histological sections, but nerves found to run in direction of cerebral ganglion from each pedal and buccal ganglion, presumably constituting missing connectives (**Figure 10B**). Pedal ganglia flattened; located ∼150 μm posterior to cerebral ganglion on both sides of foot groove (**Figures 10B,D**). Single nerve exits each ganglion medially in direction of the foot, most likely forming pedal commissure (**Figure 10D**). In posterior part of nervous system, only lateral nerve cords could be reconstructed (**Figures 10A,F**). Right lateral nerve cord thickens into swelling (**Figure 10F**, asterisk) and merges with left lateral nerve cord in suprarectal loop (**Figure 10F**).

Dorsal to pallial cavity, cuticle and underlying epidermis form protuberance (**Figures 10E,F**). Based on form, position and proximity to suprarectal loop thus interpreted as dorsoterminal sense organ, but innervation could not be detected.

Gonopericardial system

Paired gonads connected to pericardium, paired pericardioducts, a partially fused spawning duct and seminal vesicles form the reproductive system (**Figures 8B,C**, **10G–M**). Tubular, hermaphroditic gonads enclosed between midgut and dorsal body wall. Anterior region filled with oocytes (**Figures 9G**, **10J**), spermatozoids present in posterior region. Initially paired gonads fuse medially in posterior region. Connection to pericardium (=gonopericardioducts) could not be detected on histological sections (see **Figure 10I**, dotted lines). Pericardium as a flat and elongated sac delimited by thin epithelium; contains tubular heart of ∼110 μm in length (**Figures 10I** (asterisk), **K**). Posterior, pericardium widens and divides into two pericardioducts (**Figure 10L**). Two vesicles present at transition of pericardium into pericardioducts (**Figures 8B,C**, **10H,I,K**); connection between vesicles and other reproductive structures not detectable, but based on their position herein interpreted as seminal vesicles. Pericardioducts loop ventroanterior, then transition into paired spawning ducts each filled with glandular secretions (**Figures 8B,C**, **9H,I**). Spawning ducts initially paired in first half, then fusing into single duct with high columnar glandular epithelium before opening ventroanterior to hindgut into pallial cavity (**Figure 8B**).

Taxonomic remarks

Amboherpia abyssokurilensis sp. nov. is placed within Acanthomeniidae Salvini-Plawen, 1978 due to its scleritome consisting of hollow acicular needles and scale-like sclerites as well as the presence of ventrolateral foregut glands of Type *Acanthomenia* (Handl and Todt, 2005) sensu Type A (according to Salvini-Plawen, 1978a). Based on the presence of a fused vestibular-buccal cavity, radula and dorsoterminal sense organ as well as the absence of respiratory folds in the pallial cavity, the new species is assigned to the genus *Amboherpia*. *A. abyssokurilensis* sp. nov. is the third species within the genus and exhibits a combination of characters found in *A. heterotecta* Handl & Salvini-Plawen, 2002 (collected in 250–610 m in a Norwegian fjord) and *A. dolicopharyngeata* Gil-Mansilla, García-Álvarez & Urgorri, 2008 (collected in 5,389–5,415 m from the Angola Basin). Scleritome and radula resemble *A. dolicopharyngeata*, but *A. abyssokurilensis* sp. nov. differs from this species in lacking a well-developed esophagus and sphincter muscle around the spawning duct, the presence of conspicuous unicellular pharyngeal glands and a midgut with internal folds (typhlosolis) as well as the size of the base of the radula teeth.

At Stations 7–09 and 8–12 two additional specimens of an acanthomeniid lineage were collected. However, based on the available scleritome data of this lineage (**Figure 4A**) we were unable to reliably discriminate it from *A. abyssokurilensis* sp. nov. (**Figure 3F**) and we thus tentatively refer to it as Acanthomeniidae sp. 1? (see below).

Acanthomeniidae sp. 1? (Figure 4A)
Material: two specimens (ZSM Mol20170095, −96).
Distribution: Sts. 7–09, 8–12; 5,115–5,223 m.
Habitus: smooth to slightly rough appearance, ∼2 and 2.5 mm in length. Body slender, white coloration.
Scleritome: dominated by four types of acicular elements: hollow, straight with pointed distal end (**Figures 4A2,A4**) or curved with flattened distal end (**Figure 4A5**). Additionally with short, solid (?) curved needles and straight needles with ridge (**Figure 4A6**, white arrowheads). Only one type of scale visible: leaf-shaped, proximal base morphology (e.g., presence of rims) unknown (**Figure 4A3**).
Foot scales not visible.
Radula: unknown. No molecular data available.

Acanthomeniidae sp. 2 (Figure 4B):
Material: single specimen (ZSM Mol20170094).
Distribution: St. 8–12, 5,115–5,124 m.
Habitus: smooth appearance, 6.5 mm in size; body slender, yellow coloration (**Figure 4B**).
Scleritome: dominated by two types of hollow, acicular elements: curved with pointed distal end (**Figure 4B3**) and straight (**Figure 4B4**). Five types of scales: slightly concave, with pointed distal end (**Figure 4B1**), excavated scales with drawn-out, sharp distal end (75 μm) [**Figure 4B5** (1)], scales with small stalk and rim at proximal base of (25–35 μm) [**Figure 4B5** (2)], pointed rod-shaped scales with strongly thickened lateral ridges and flat back (25 μm) [**Figures 4B2, B5** (3)], excavated blade-shaped scales [**Figure 4B5** (4)]. Foot scales blade-shaped with bulge (60 μm length) [**Figure 4B** (5)].
Taxonomic remarks: this lineages is similar to the other acanthomeniids in its habitus (compare **Figures 4A,B**) as well as in some distinct scleritome characters, such as the presence of hollow, straight needles (**Figures 4A2,B3**) and scales with a small stalk and rimmed proximal base [compare **Figure 4B5** (1, 2) with Figure 2D (14–16, 19) in Scheltema (1999) and Figure 2 in Handl and Salvini-Plawen (2002)]. Radula: unknown. No molecular data available.

STERROFUSTIA Salvini-Plawen, 1978

Order characterized by the presence of only solid acicular sclerites, which can be combined with various types of solid scales.

Sterrofustia sp. 1 (Figure 4C):
Material: single specimen (ZSM Mol20170108).
Distribution: St. 11–12, 5,348–5,350 m.
Habitus: furry appearance due to perpendicularly projecting sclerites, 2.7 mm long; white coloration (**Figure 4C**). Scleritome: dominated by solid acicular elements of varying length (150–250 μm) distributed evenly across the body [**Figures 4C1,C4** (1)]; cross-section like a three-point star (**Figure 4C2**, white arrowhead), second type of solid elements as interspersed straight needles [**Figure 4C4** (3). Keeled scales up to 150 μm in length (**Figure 4C4** (2)]. Foot scales blade-shaped (75 μm length) [**Figure 4C4** (4)].
Radula: unknown. No molecular data available.

PHOLIDOSKEPIA Salvini-Plawen, 1978

This order is characterized by almost exclusively scaly sclerites and only occasional acicular elements. Only one family of this order was represented in our material by three distinct lineages.

Dondersiidae Simroth, 1893
The scleritome of dondersiids consists of various types of scales, occasionally combined with solid acicular elements. Based on this combination of scleritome elements (scales together with solid needles) the following three lineages were assigned to Dondersiidae.

Dondersiidae sp. 1 (Figure 4D):
Material: single specimen (ZSM Mol20170106).
Distribution: St. 6–12, 5,291–5,307 m.
Habitus: velvety, with sclerites arranged flat against body surface; ∼3 mm in length; yellow coloration (**Figure 4D**).
Scleritome: dominated by leaf-shaped scales with rimmed base (up to 30 μm) (**Figures 4D1,D3**).
Acicular elements interspersed, solid short needles (up to 60 μm) (**Figures 4D1,D2**). No information on foot scales. Surface of all sclerites with hair-like ultrastructure (**Figure 4D3**).
Radula: unknown. No molecular data available.

Dondersiidae sp. 2 (Figure 4E):
Material: single specimen (ZSM Mol20170107).
Distribution: St. 8–12, 5,115–5,124 m.
Habitus: smooth, ∼3.5 mm in length; white coloration (**Figure 4E**).
Scleritome: dominated by scales in leaf-shaped form [**Figures 4E2,E4** (1)]; leaf-shaped scales with short stalk [**Figure 4E4** (2)]; scales with diamond shape [**Figure 4E4** (3)]; elongated, slender scales with stalk [**Figure 4E4**, (4)]. Interspersed solid short [**Figure 4E3** white arrowheads, **Figure 4E4** (5)] and long needles (up to 100 μm in length) [**Figures 4E3,E4** (6)]. No information on foot scales.
Taxonomic remarks: the scleritome of Dondersiidae sp. 2, especially the stalked elements [**Figure 4E4** (2, 4)], is highly similar to the Antarctic *Nematomenia* (?) *squamosa* (Thiele, 1913) (see Figure 29 in Salvini-Plawen, 1978a).
Radula: unknown. No molecular data available.

Dondersiidae sp. 3 (Figure 5):
Material: single specimen (ZSM Mol20170105).
Distribution: St. 7–09, 5,216–5,223m.
Habitus: spiny, with several conspicuously longer acicular elements; ca. 780 μm in size; white coloration (**Figure 5A**).
Scleritome: three types of scale-like, solid elements. Main type: symmetrically leaf-shaped, with median keel (∼40 μm length) (**Figure 5A5**), second type only found anterior, leaf-shaped but with strongly rimmed base and lateral ridge (12 μm) (**Figure 5A4**), and flat leaf-shaped scales (40 μm) (**Figure 5A6**). Two types of hollow, needle-like elements interspersed between scales at lateral and dorsal sides. Curved ones with circular diameter (up to 200 μm length) (**Figure 5A3**). At posterior end: second type of acicular sclerites with strong median keel; length: up to 200 μm (**Figures 5A1,A2**); unknown whether solid or

hollow. No information on foot scales. Radula: unknown. No molecular data available.

Taxonomic remarks: within Dondersiidae the encountered lineage bears some similarities to *Helluoherpia aegiri* Handl & Büchinger, 1996 in the presence of distinctively rimmed and flat scales as well as solid needles. However, there are some distinct differences i.e., the presence of medially keeled scales in Dondersiidae sp. 3 (**Figure 5A5**) which are lacking in *H. aegiri* (Handl and Büchinger, 1996).

DISCUSSION

Combining Scleritome Morphology and Barcodes: A Fast and Efficient Approach to Assess Solenogaster Diversity

Solenogastres are usually excluded from biodiversity assessments due to the complex and time-consuming methods necessary for their taxonomic identification. While most solenogaster taxonomists have focused on species delineation based on microanatomical and histological characters (Nierstrasz, 1902; Heath, 1911; Salvini-Plawen, 1978a,b), Scheltema and Schander (2000) already highlighted the value of habitus and scleritome for species delineation and phylogeny. Solenogaster external morphology provides a character set which is easily accessible via light microscopy, and since its analysis does not require more taxonomic training than morphological species delineation in other clades, it is also feasible for non-specialists.

Our study identifies at least 19 morphospecies, which can be distinctively delineated based on the differences in their scleritomes. Methodologically, light microscopy is sufficient to characterize the overall diversity of the scleritome. Scanning electron microscopy (SEM) on entire specimens, however, provides a better overview on the distribution of sclerites as well as additional ultrastructural information (see, e.g., **Figure 4A6**). However, SEM of entire individuals needs to be combined with investigation of isolated sclerites, as their base might also provide important taxonomic characters. Scleritome-based species delineation might become limited, however, with denser sampling and when dealing with closely related lineages. We were unable, for example, to reliably discriminate Acanthomeniidae sp. 1? (**Figure 4A**) from *A. abyssokurilensis* sp. nov. (**Figure 3F**) based on the available scleritome data. Knowledge on the intraspecific variation of the scleritome is generally scarce, but in some families, as e.g., Epimeniidae (Cavibelonia), the slight interspecific variability is overlapped by intraspecific variability (Salvini-Plawen, 1997a). So far, species boundaries in Solenogastres have never been tested via molecular markers. Especially variability of sclerite size is difficult to evaluate with regard to its taxonomic value, without knowledge on the maturity of the individual, as can only be derived from histological sectioning. Moreover, in minute mesopsammic Solenogastres externally cryptic and co-occurring species have been documented (Bergmeier et al., 2016a), and crypsis might be a common phenomenon also among deep-sea Solenogastres. Thus, scleritome-based species delineation needs to be combined with molecular approaches.

Nuclear genes of Solenogastres are notoriously hard to amplify due to complex secondary structures, which inhibit amplification via standard PCR (Meyer et al., 2010). Using the mitochondrial standard markers for cytochrome *c* oxidase subunit 1 and 16 S rRNA broadly applied on various clades of molluscs (e.g., Klussmann-Kolb et al., 2008; Wilson et al., 2010; Stöger et al., 2013; Kano et al., 2016) resulted in low amplification success. In general, successful DNA amplification of these deep-sea molluscs is dependent on fast processing of the material. After 2.5 years of storage in ethanol, the success rate dropped considerably in comparison to fresh material (own observations). Using a solenogaster-specific pair of self-designed primers ("16Soleno-f" and "–r," see section Materials and Methods) increased our amplification success of mitochondrial 16S rRNA, and we were at least able to generate sequence data for ∼50% of our material.

Our molecular dataset (in conjunction with the provided scleritome data) will allow to reliably assign novel material collected in the region to our herein preliminary characterized morphospecies. The comparably high (i.e., >16%) genetic distances on the 16S rRNA sequences between the identified morphospecies at present supports the hypothesis of them being independently evolving lineages. Due to the low number of sequences of genetically distant lineages within this worm-mollusc clade with hypothesized Paleozoic origin (Vinther et al., 2012), our barcode dataset currently does not allow for meaningful molecular species delineation. Tree-based approaches (as, e.g., GMYC; Pons et al., 2006; Monaghan et al., 2009) analyzing the transition point between the speciation and coalescent processes on an ultrametric gene tree are largely hampered by the inclusion of singletons (80% in our dataset). Bayesian species delineations (Yang and Rannala, 2010; Zhang et al., 2011) rely on multiple loci, but have nevertheless been criticized for reconstructing structure in a dataset but not necessarily species, unable to discriminate between population and speciation processes (Sukumaran and Knowles, 2017). A denser sampling of abyssal Solenogastres and a multi marker molecular approach is needed to investigate the species boundaries between deep-sea Solenogastres.

An advantage of our workflow is the efficient and fast assessment of operational taxonomic units and therein providing valuable information on α-diversity. The generated molecular barcodes (though unfortunately incomplete) allow for fast and reliable assignment of future material to the identified lineages. Low success rates in direct amplification via PCR on older material might be circumvented by high throughput sequencing approaches resulting in more significant datasets for molecular species delineation. External morphology links amplified barcodes to the established taxonomic system of the clade: ∼75% of lineages in our study could be assigned to family level and beyond. For four lineages [Cavibelonia sp. 1, sp. 2 (both **Figure 2**), sp. 3 (**Figure 3A**) and sp. 4 (**Figure 3B**) and Sterrofustia sp. 1 (**Figure 4C**)] taxonomic placement was impossible, despite detailed documentation of their scleritomes. Unique and conspicuous sclerites, such as the three-point star needles in Sterrofustia sp. 1 (**Figure 4C2**), never documented before in Solenogastres, suggest that these lineages are new to science and thus currently cannot be integrated into the existing

classificatory system. Singletons like Sterrofustia sp. 1 could be easily excluded from traditional approaches, underlining the value of an overall characterization of α-diversity, which helps to identify key lineages of major evolutionary importance for future work and at the same time provides full formal species descriptions in common lineages.

Systematics and Diversity of Abyssal Solenogastres in the Northwest Pacific

The current state of knowledge regarding solenogaster species diversity in the region is generally scarce with hitherto only 11 known species prior to this study. Nine have been described and reported from the coastal waters off Japan, one of them—*Alexandromenia marisjaponica* Saito & Salvini-Plawen, 2014 (Amphimeniidae)—from the Sea of Japan and the others from the Pacific coast [*Neomenia yamamotoi* Baba, 1975 (Neomeniidae), *Epimenia ohshimai* Baba, 1940 and *E. babai* Salvini-Plawen, 1997 (Epimeniidae), *Anamenia triangularis* (Heath, 1911), *A. amabilis* Saito & Salvini-Plawen, 2010 and *A. farcimen* (Heath, 1911) and *Strophomenia ophidiana* Heath, 1911 (all Strophomeniidae), and *Driomenia pacifica* Heath, 1911 (Rhopalomeniidae)] (see Baba, 1940, 1975; Saito and Salvini-Plawen, 2010, 2014). Two species are known from the Sea of Okhotsk (*Neomenia yamamotoi* and *Halomenia gravida* Heath, 1911) and one from the Bering Sea [*Nematomenia platypoda* (Heath, 1911), Dondersiidae] (García-Álvarez and Salvini-Plawen, 2007; Sirenko, 2013). All of these species were collected from 40 to 1,500 m, while the Northwest Pacific lower bathyal and beyond remains largely unexplored with regard to solenogaster fauna. Our sampling of the abyssal Northwest Pacific (NWP) Plain, close to the Kuril-Kamchatka Trench, revealed 19 distinct solenogaster lineages (excluding Acanthomeniidae sp. 1?), which were delimited based on a combination of external morphology, molecular sequence data and microanatomy. Of the five families identified in our study, only Dondersiidae and Pruvotinidae have already been reported from the NWP region (*N. platypoda* from the Bering Sea and *H. gravida*). Based on distinct differences in habitus (*N. platypoda* has a distinct dorsal keel, see plate 1, Figure 4 in Heath, 1911), scleritome (and in case of Halomeniinae sp. 1 also anatomy) as well as bathymetric differences of more than 4,000 m, conspecifity between *N. platypoda*, *H. gravida* and any of the five pruvotinid and dondersiid lineages uncovered in this study can be excluded, and we assume that all 19 abyssal lineages present novel records for this region. The diversity of Solenogastres in the Northwest Pacific and its marginal seas is thus almost tripled to 30 recorded species.

The only sterrofustian lineage Sterrofustia sp. 1 found during the KuramBio cruise presents the first record of this order in the Northwest Pacific. For the discovered cavibelonian lineages (except Pruvotinidae, see above), the geographically closest records of Proneomeniidae are from Hawaii and the Indonesian Sunda Sea (Heath, 1911), and Simrothiellidae have been described from the Atacama Trench and hot-vent sites on the East Pacific Rise (Scheltema and Kuzirian, 1991; Scheltema, 2000; Salvini-Plawen, 2008). Proneomeniidae sp. 1, Simrothiellidae sp. 1 and sp. 2 expand the potential distribution ranges of the two families to the Northwest Pacific, and besides the West Indian Ocean, the simrothiellid genus *Spiomenia* is for the first time reported from the Pacific. The known distribution range of this family now covers the North and South Atlantic and the Antarctic Davis Straight as well as the Northwest Pacific. The discovery of *A. abyssokurilensis* sp. nov. expands the known distribution range of the genus from the abyssal Angola Basin (5,300–5,500 m) in the Southern Atlantic and Norwegian fjords (250–610 m) to the abyssal plain of the Northwest Pacific (5,390–5,400 m; Handl and Salvini-Plawen, 2002; Gil-Mansilla et al., 2008).

Little is known about vertical and horizontal distribution ranges of Solenogastres. While some pruvotinid and proneomeniid Solenogastres are brooders (Heath, 1911; Salvini-Plawen, 1978a; Todt and Kocot, 2014) with low distribution ranges, the majority of species develops via lecitotrophic, planktonic larvae. Between 5 and 11 days of swimming behavior from hatching to settlement of larvae have been observed (Okusu, 2002; Todt and Wanninger, 2010) for some clades and longer larval survival periods can be assumed for deep-sea lineages in cold waters. Due to the different modes in development, the dispersal abilities between the different clades might be highly variable and wide distribution ranges as commonly found in many deep-sea taxa cannot be excluded.

The majority of the discovered lineages from the Northwest Pacific presents unique scleritome characters distinguishable from other described abyssal lineages, and likely are species new to science. Only the acanthomeniid *Veromenia* cf. *singula* was identified in our material based on external similarities and the lack of any anatomical features distinguishing it from the individuals described from the abyssal Angola Basin (see Figures 4E,F, 5 in Gil-Mansilla et al., 2008). Comparative molecular data from the Atlantic material is needed to clarify the relationship between the Atlantic and Pacific *Veromenia* lineages and to gain valuable insights on the distribution patterns of abyssal Solenogastres. Currently, available data is sufficient to present the discovered diversity of abyssal Solenogastres from the NWP plain; however, the collected material and thereof retrieved data is insufficient to provide formal species descriptions within the present classificatory system on all discovered lineages. A combination of scleritome and molecular characters will likely be most suitable for rapid species description in the future, this is still hampered at present, however, by a largely histology-based classificatory system. Molecular data from type material of the established lineages is needed to avoid creating a parallel taxonomic system for Solenogastres (Jörger, 2015).

A First Glimpse into the Abyssal Solenogaster Fauna—All Lost Loners?

The Mediterranean and the Eastern Atlantic off the European coast constitute relatively well-studied regions in terms of solenogaster fauna, harboring nearly 30% of the global solenogaster diversity (Salvini-Plawen, 1997b; García-Álvarez et al., 2014; Pedrouzo et al., 2014). Intensive taxonomic work has also been conducted around Antarctica (Salvini-Plawen, 1978a,b; García-Álvarez et al., 1998, 2009; Zamarro et al., 2012), resulting

in close to 45% of the described global species diversity. In general, sampling has so far largely focused on bathyal depths and the only comparable study on Solenogastres from similar depths has been carried out in the South Atlantic Angola Basin (DIVA-1 expedition, Arbizu and Schminke, 2005): half of the globally known 18 species (classified in five families and 11 genera) described from below 4,000 m were collected here. While almost all previously known lineages belong to the order Cavibelonia (except for two), our study adds the first record of an abyssal sterrofustian lineage and doubles the global number of solenogaster lineages discovered in the abyss.

The solenogaster fauna of the abyssal Angola Basin and the Northwest Pacific Plain are dominated by cavibelonian Simrothiellidae, Acanthomeniidae and Pruvotinidae—with three identified genera (*Spiomenia*, *Amboherpia,* and *Veromenia*) present in both regions. From the NWP plain we collected 33 specimens, after sampling 53,708 m^2 of sea-floor with the C-EBS (Brandt et al., 2015) resulting in 19 morphospecies assigned to at least five different families, with a high number of singletons (74%). EBS sampling of only half the area of sea-floor in the Angola Basin (27,765 m^2, see Brandt et al., 2005) yielded twice as many specimens (64 individuals) and 50% more species (30 spp.) (Gil-Mansilla, 2008; Gil-Mansilla et al., 2008, 2009, 2012), indicating an overall higher diversity and abundance of Solenogastres in the region. The spatial distribution of Solenogastres is patchy in both regions. This patchiness seems to be more pronounced in the Angola Basin, where either only single specimens or between 10 and 23 individuals were sampled (Gil-Mansilla, 2008). In the NWP individual numbers from neighboring C-EBS hauls are continuously low (see **Table 1**). Distributional patchiness has been observed for several deep-sea taxa including molluscs (Schwabe et al., 2007; Jörger et al., 2014), and is generally linked to the heterogeneity of habitats and the availability of food sources (Rex and Etter, 2010; McClain et al., 2011). The majority of Solenogastres are predators of anthozoan or hydrozoan cnidarians (Salvini-Plawen, 1981), and their occurrence might thus be connected to the presence of their preferred prey.

The observed rarity of the discovered abyssal Solenogastres might be an indication for source-sink mechanics, in which the low density of individuals prevents the sustainability of populations of sexually reproducing organisms and the impoverished abyssal fauna is dependent on larval influx of bathyal populations (Rex et al., 2005). Preliminary diversity assessments indicate differences in the taxonomic composition of the shallower Kuril basin in the semi-isolated Sea of Okhotsk and the abyssal fauna investigated herein with only few conspecifics (Ostermair et al., accepted). Comparative analyses of the bathyal solenogaster diversity of the eastern slopes of the Kuril Islands and intensified sampling in the area are necessary to evaluate the origin of the abyssal NWP fauna, whether they present lost loners in the abyss or belong to reproducing abyssal populations.

AUTHOR CONTRIBUTIONS

FB: conducted the morphological and molecular analyses and drafted the manuscript; AB: organized the KuramBio expedition; ES: collected and sorted the KuramBio material; KJ: designed the study. All authors contributed to and approved the final version of the manuscript.

FUNDING

The study was funded by a Student Research Grant from the Malacological Society of London to FB and DFG grant JO-1311 to KJ. We are grateful for the financial support through the grant 03G0223A by the German Federal Ministry of Education and Research (PTJ). Publication was supported by an article waiver from "Frontiers in Marine Science" to FB, awarded during the Deep-Sea Biology Symposium 2015 in Aveiro (Portugal).

ACKNOWLEDGMENTS

Thanks are due to the Captain and the crew for help on board as well as to all scientists joining the expedition of the R/V *Sonne* for collecting material for the present study. We are also grateful to Heidemarie Gensler for her support during histological sectioning and Lukas Ostermair and Dominik Kammerer for digitalization of histological serial sections. We would like to thank the two reviewers for their valuable comments and suggestions which improved the manuscript. This is KuramBio publication #39.

REFERENCES

Allen, J. A. (2008). Bivalvia of the deep Atlantic. *Malacologia* 50, 57–173. doi: 10.4002/0076-2997-50.1.57

Arbizu, P. M., and Schminke, H. K. (2005). DIVA-1 expedition to the deep sea of the Angola Basin in 2000 and DIVA-1 workshop in 2003. *Organ. Divers. Evol.* 5, 1–2. doi: 10.1016/j.ode.2004.11.009

Baba, K. (1940). *Epimenia ohshimai* a new solenogastre species from Amakusa, Japan. *Venus* 10, 91–96.

Baba, K. (1975). *Neomenia yamamotoi* spec. nov., a gigantic Solenogaster (Mollusca: Class Solenogastres, Family Neomeniidae), occurring in the north-eastern part of Japan. *Publ. Seto Mar. Biol. Lab.* 22, 277–284. doi: 10.5134/175901

Belyaev, G. (1983). *Investigation of Ultraabyssal Fauna. Research Vessel "Vitjaz" and Her Expeditions 1949–1979*. Moscow: Nauka.

Bergmeier, F. S., Haszprunar, G., Todt, C., and Jörger, K. M. (2016a). Lost in a taxonomic Bermuda Triangle: comparative 3D-microanatomy of cryptic mesopsammic Solenogastres (Mollusca). *Organ. Divers. Evol.* 16, 613–639. doi: 10.1007/s13127-016-0266-6

Bergmeier, F. S., Melzer, R. R., Haszprunar, G., and Jörger, K. M. (2016b). Getting the most out of minute singletons: molecular data from SEM-samples in Solenogastres (Mollusca). *Malacologist* 66, 23–25.

Bouchet, P., and Warén, A. (1980). Revision of the northeast Atlantic bathyal and abyssal Turridae (Mollusca, Gastropoda). *J. Molluscan Stud.* 46, 1–119. doi: 10.1093/mollus/46.Supplement_8.1

Brandt, A., Brenke, N., Andres, H.-G., Brix, S., Guerrero-Kommritz, J., Mühlenhardt-Siegel, U., et al. (2005). Diversity of peracarid crustaceans (Malacostraca) from the abyssal plain of the Angola Basin. *Organ. Divers. Evol.* 5, 105–112. doi: 10.1016/j.ode.2004.10.007

Brandt, A., Elsner, N., Brenke, N., Golovan, O., Malyutina, M., Riehl, T., et al. (2013). Epifauna of the Sea of Japan collected via a new epibenthic sledge equipped with camera and environmental sensor systems. *Deep Sea Res. Part 2 Top. Stud. Oceanogr.* 86, 43–55. doi: 10.1016/j.dsr2.2012.07.039

Brandt, A., Elsner, N. O., Malyutina, M. V., Brenke, N., Golovan, O. A., Lavrenteva, A. V., et al. (2015). Abyssal macrofauna of the Kuril–Kamchatka Trench area (Northwest Pacific) collected by means of a camera–epibenthic sledge. *Deep Sea Res. Part. 2 Top. Stud. Oceanogr.* 111, 175–187. doi: 10.1016/j.dsr2.2014.11.002

Brandt, A., Gooday, A. J., Brandão, S. N., Brix, S., Brökeland, W., Cedhagen, T., et al. (2007). First insights into the biodiversity and biogeography of the Southern Ocean deep sea. *Nature* 447, 307–311. doi: 10.1038/nature05827

Brandt, A., and Malyutina, M. (2012). The German-Russian deep-sea expedition KuramBio (Kurile Kamchatka Biodiversity Study): to the Kurile Kamchatka Trench and abyssal plain on board of the R/V Sonne, 223rd Expedition. [*Online Cruise Report*]. doi: 10.2314/GBV:741102293

Brault, S., Stuart, C. T., Wagstaff, M. C., McClain, C. R., Allen, J. A., and Rex, M. A. (2013). Contrasting patterns of alpha- and beta-diversity in deep-sea bivalves of the eastern and western North Atlantic. *Deep Sea Res. Part. 2 Top. Stud. Oceanogr.* 92, 157–164. doi: 10.1016/j.dsr2.2013.01.018

Castresana, J. (2000). Selection of conserved blocks from multiple alignments for their use in phylogenetic analysis. *Mol. Biol. Evol.* 17, 540–552. doi: 10.1093/oxfordjournals.molbev.a026334

Cobo, M. C., Pedrouzo, L., García-Álvarez, O., Barrio, L., Urgorri, V., and Cobo, F. (2013). "Contribution to abyssal Angola Basin Solenogastres (Mollsuca) with preliminary records of two species of the order Pholidoskepia," in *World Congress of Malacology* (Ponta Delgada; Azores: Acoreana), 162.

Danovaro, R., Company, J. B., Corinaldesi, C., D'Onghia, G., Galil, B., Gambi, C., et al. (2010). Deep-sea biodiversity in the Mediterranean Sea: the known, the unknown, and the unknowable. *PLoS ONE* 5:e11832. doi: 10.1371/journal.pone.0011832

Gage, J. D., and Tyler, P. A. (1991). *Deep-Sea Biology: A Natural History of Organisms at the Deep-Sea Floor*. Cambridge: Cambridge University Press.

García-Álvarez, O., and Salvini-Plawen, L. V. (2007). Species and diagnosis of the families and genera of Solenogastres (Mollusca). *Iberus* 25, 73–143.

García-Álvarez, O., Salvini-Plawen, L. V., Urgorri, V., and Troncoso, J. S. (2014). *Fauna Ibérica Vol. 38, Mollusca: Solenogastres, Caudofoveata, Monoplacophora*. Madrid: Museo Nacional De Ciencias Naturales, CSIC.

García-Álvarez, O., Urgorri, V., and Salvini-Plawen, L. V. (1998). *Dorymenia troncosoi* sp. nov. (Mollusca Solenogastres: Proneomeniidae), a new species from the South Shetland Islands (Antarctica). *Polar Biol.* 20, 382–387. doi: 10.1007/s003000050318

García-Álvarez, O., Zamarro, M., and Urgorri, V. (2009). Proneomeniidae (Solenogastres, Cavibelonia) from the Bentart-2006 Expedition, with description of a new species. *Iberus* 27, 67–78.

Gil-Mansilla, E. (2008). *Los Moluscos Solenogastros de la Campa-a DIVA 1 en la Cuenca Abisal de Angola*. dissertation. Universidade de Santiago de Compostela.

Gil-Mansilla, E., García-Álvarez, O., and Urgorri, V. (2008). New Acanthomeniidae (Solenogastres, Cavibelonia) from the abyssal Angola Basin. *Zootaxa* 1866, 175–186.

Gil-Mansilla, E., García-Álvarez, O., and Urgorri, V. (2009). A new genus and two new species of Simrothiellidae (Solenogastres: Cavibelonia) from the Abyssal Angola Basin. *J. Mar. Biol. Assoc. U.K.* 89, 1507–1515. doi: 10.1017/S0025315409000666

Gil-Mansilla, E., García-Álvarez, O., and Urgorri, V. (2012). Three new species of *Kruppomenia* (Solenogastres: Simrothiellidae) from the abyssal Angola Basin. *J. Mar. Biol. Assoc. U.K.* 92, 349–359. doi: 10.1017/S0025315411001275

Girard, F., Lacharité, M., and Metaxas, A. (2016). Colonization of benthic invertebrates in a submarine canyon in the NW Atlantic. *Mar. Ecol. Prog. Ser.* 544, 53–64. doi: 10.3354/meps11555

Glaubrecht, M., Maitas, L., and Salvini-Plawen, L. V. (2005). Aplacophoran Mollusca in the Natural History Museum Berlin. An annotated catalogue of Thiele's type specimens, with a brief review of "Aplacophora" classification. *Zoosyst. Evol.* 81, 145–166. doi: 10.1002/mmnz.200510009

Gutt, J., Alvaro, M., Barco, A., Böhmer, A., Bracher, A., David, B., et al. (2016). Macroepibenthic communities at the tip of the Antarctic Peninsula, an ecological survey at different spatial scales. *Polar Biol.* 39, 829–849. doi: 10.1007/s00300-015-1797-6

Handl, C. H., and Büchinger, T. (1996). *Helluoherpia aegiri* gen. n. et sp. n. aus Norwegen (Mollusca: Solenogastres: Dondersiidae). *Ann. Naturhist. Mus. Wien* 98, 65–70.

Handl, C. H., and Salvini-Plawen, L. V. (2002). New records of Solenogastres - Cavibelonia (Mollusca) from Norwegian fjords and shelf waters including three new species. *Sarsia* 87, 423–450. doi: 10.1080/0036482021000155725

Handl, C. H., and Todt, C. (2005). Foregut glands of Solenogastres (Mollusca): anatomy and revised terminology. *J. Morphol.* 265, 28–42. doi: 10.1002/jmor.10336

Heath, H. (1911). Reports on the scientific results of the expedition to the Tropical Pacific, in charge of Alexander Agassiz, by the U. S. Fish Commission Steamer Albatross, from August 1899 to June 1900, Commander Jefferson F. Moser. XVI. The Solenogastres. *Mem. Mus. Comp. Zoology Harv. Coll.* 45, 1–182.

Hortal, J., de Bello, F., Diniz-Filho, J. A. F., Lewinsohn, T. M., Lobo, J. M., and Ladle, R. J. (2015). Seven shortfalls that beset large-scale knowledge of biodiversity. *Annu. Rev. Ecol. Evol. Syst.* 46, 523–549. doi: 10.1146/annurev-ecolsys-112414-054400

Jörger, K. M. (2015). "The potential of museomics to revitalize the taxonomy of acplacophoran molluscs," in *108th Annual Meeting of the German Zoological Society* (Graz), 115.

Jörger, K. M., Schrödl, M., Schwabe, E., and Würzberg, L. (2014). A glimpse into the deep of the Antarctic Polar Front – Diversity and abundance of abyssal molluscs. *Deep Sea Res. Part. 2 Top. Stud. Oceanogr.* 108, 93–100. doi: 10.1016/j.dsr2.2014.08.003

Kano, Y., Brenzinger, B., Nützel, A., Wilson, N. G., and Schrödl, M. (2016). Ringiculid bubble snails recovered as the sister group to sea slugs (Nudipleura). *Sci. Rep.* 6:30908. doi: 10.1038/srep30908

Klussmann-Kolb, A., Dinapoli, A., Kuhn, K., Streit, B., and Albrecht, C. (2008). From sea to land and beyond-new insights into the evolution of euthyneuran Gastropoda (Mollusca). *BMC Evol. Biol.* 8:57. doi: 10.1186/1471-2148-8-57

McClain, C. R., and Hardy, S. M. (2010). The dynamics of biogeographic ranges in the deep sea. *Proc. R. Soc. B Biol. Sci.* 277, 3533–3546. doi: 10.1098/rspb.2010.1057

McClain, C. R., Nekola, J. C., Kuhnz, L., and Barry, J. P. (2011). Local-scale faunal turnover on the deep Pacific seafloor. *Mar. Ecol. Prog. Ser.* 422, 193–200. doi: 10.3354/meps08924

Meyer, A., Todt, C., Mikkelsen, N. T., and Lieb, B. (2010). Fast evolving 18S rRNA sequences from Solenogastres (Mollusca) resist standard PCR amplification and give new insights into mollusk substitution rate heterogeneity. *BMC Evol. Biol.* 10, 1–12. doi: 10.1186/1471-2148-10-70

Miller, M. A., Pfeiffer, W., and Schwartz, T. (2010). "Creating the CIPRES Science Gateway for inference of large phylogenetic trees," in *Gateway Computing Environments Workshop (GCE)*, IEEE, 1–8.

Monaghan, M. T., Wild, R., Elliot, M., Fujisawa, T., Balke, M., Inward, D. J., et al. (2009). Accelerated species inventory on Madagascar using coalescent-based models of species delineation. *Syst. Biol.* 58, 298–311. doi: 10.1093/sysbio/syp027

Nierstrasz, H. F. (1902). *The Solenogastres of the Siboga-Expedition*. Leiden: EJ Brill.

Okusu, A. (2002). Embryogenesis and development of *Epimenia babai* (Mollusca Neomeniomorpha). *Biol. Bull.* 203, 87–103. doi: 10.2307/1543461

Ostermair, L., Brandt, A., Haszprunar, G., Jörger, K. M., and Bergmeier, F. S. (accepted). First insights into the solenogaster diversity of the Sea of Okhotsk with the description of a new species of *Kruppomenia* (Simrothiellidae, Cavibelonia). *Deep Sea Res. Part. 2 Top. Stud. Oceanogr.*

Pedrouzo, L., Cobo, M. C., García-Álvarez, O., Rueda, J. L., Gofas, S., and Urgorri, V. (2014). Solenogastres (Mollusca) from expeditions off the South Iberian Peninsula, with the description of a new species. *J. Nat. Hist.* 48, 2985–3006. doi: 10.1080/00222933.2014.959576

Pons, J., Barraclough, T. G., Gomez-Zurita, J., Cardoso, A., Duran, D. P., Hazell, S., et al. (2006). Sequence-based species delimitation for the DNA taxonomy of undescribed insects. *Syst. Biol.* 55, 595–609. doi: 10.1080/10635150600852011

Posada, D. (2008). jModelTest: phylogenetic model averaging. *Mol. Biol. Evol.* 25, 1253–1256. doi: 10.1093/molbev/msn083

Qiu, B. (2001). "Kuroshio and Oyashio Currents," in *Ocean Currents: A Derivative of the Encyclopedia of Ocean Sciences*, eds J. H. Steele, S. A. Thorpe, and K. K. Turekian (Oxford: Academic Press), 1423–1425. doi: 10.1006/rwos.2001.0350

Ramirez-Llodra, E., Brandt, A., Danovaro, R., De Mol, B., Escobar, E., German, C., et al. (2010). Deep, diverse and definitely different: unique attributes of the world's largest ecosystem. *Biogeosciences* 7, 2851–2899. doi: 10.5194/bg-7-2851-2010

Rex, M. A. (1973). Deep-sea species diversity: decreased gastropod diversity at abyssal depths. *Science* 181, 1051–1053. doi: 10.1126/science.181.4104.1051

Rex, M. A., and Etter, R. J. (2010). *Deep-Sea Biodiversity: Pattern and Scale*. Cambridge, MA: Harvard University Press.

Rex, M. A., Etter, R. J., Morris, J. S., Crouse, J., McClain, C. R., Johnson, N. A., et al. (2006). Global bathymetric patterns of standing stock and body size in the deep-sea benthos. *Mar. Ecol. Prog. Ser.* 317, 1–8. doi: 10.3354/meps317001

Rex, M. A., McClain, C. R., Johnson, N. A., Etter, R. J., Allen, J. A., Bouchet, P., et al. (2005). A source-sink hypothesis for abyssal biodiversity. *Am. Nat.* 165, 163–178. doi: 10.1086/427226

Richardson, K., Jarett, L., and Finke, E. (1960). Embedding in epoxy resins for ultrathin sectioning in electron microscopy. *Stain Technol.* 35, 313–323. doi: 10.3109/10520296009114754

Román, S., Vanreusel, A., Romano, C., Ingels, J., Puig, P., Company, J. B., et al. (2016). High spatiotemporal variability in meiofaunal assemblages in Blanes Canyon (NW Mediterranean) subject to anthropogenic and natural disturbances. *Deep Sea Res. Part. 1 Oceanogr. Res. Pap.* 117, 70–83. doi: 10.1016/j.dsr.2016.10.004

Ruthensteiner, B. (2008). Soft Part 3D visualization by serial sectioning and computer reconstruction. *Zoosymposia* 1, 63–100. doi: 10.11646/zoosymposia.1.1.8

Saito, H., and Salvini-Plawen, L. V. (2010). A new species of *Anamenia* (Mollusca: Solenogastres: Cavibelonia) from southern Japan. *Venus* 69, 1–15.

Saito, H., and Salvini-Plawen, L. V. (2014). A new deep-sea Solenogastres (Mollusca) from the Sea of Japan. *Natl. Mus. Nat. Sci.* 44, 39–54.

Salvini-Plawen, L. V. (1978a). Antarktische und subantarktische Solenogastres. Eine Monographie 1898–1974 (Part 1). *Zoologica* 44, 1–155.

Salvini-Plawen, L. V. (1978b). Antarktische und subantarktische Solenogastres. Eine Monographie 1898–1974 (Part 2). *Zoologica* 44, 157–315.

Salvini-Plawen, L. V. (1981). The molluscan digestive system in evolution. *Malacologia* 21, 371–401.

Salvini-Plawen, L. V. (1997a). Systematic revision of the Epimeniidae (Mollusca: Solenogastres). *J. Molluscan Stud.* 63, 131–155. doi: 10.1093/mollus/63.2.131

Salvini-Plawen, L. V. (1997b). Fragmented knowledge on West-European and Iberian Caudofoveata and Solenogastres. *Iberus* 15, 35–50.

Salvini-Plawen, L. V. (2008). Three new species of Simrothiellidae (Solenogastres) associated with the hot-vent biotope. *J. Molluscan Stud.* 74, 223–238. doi: 10.1093/mollus/eyn010

Scheltema, A. H. (1999). New eastern Atlantic neomenioid aplacophoran molluscs (Neomeniomorpha, Aplacophora). *Ophelia* 51, 1–28. doi: 10.1080/00785326.1999.10409397

Scheltema, A. H. (2000). Two new hydrothermal vent species, *Helicoradomenia bisquama* and *Helicoradomenia acredema*, from the eastern Pacific Ocean (Mollusca, Aplacophora). *Argonauta* 14, 15–25.

Scheltema, A. H., and Kuzirian, A. (1991). *Helicoradomenia juani* gen. et sp. nov., a Pacific hydrothermal vent Aplacophora (Mollusca: Neomeniomorpha). *Veliger* 34, 195–203.

Scheltema, A. H., and Schander, C. (2000). Discrimination and phylogeny of solenogaster species through the morphology of hard parts (Mollusca, Aplacophora, Neomeniomorpha). *Biol. Bull.* 198, 121–151. doi: 10.2307/1542810

Schrödl, M., Bohn, J. M., Brenke, N., Rolán, E., and Schwabe, E. (2011). Abundance, diversity, and latitudinal gradients of southeastern Atlantic and Antarctic abyssal gastropods. *Deep Sea Res. Part. 2 Top. Stud. Oceanogr.* 58, 49–57. doi: 10.1016/j.dsr2.2010.10.009

Schwabe, E., Bohn, J. M., Engl, W., Linse, K., and Schrödl, M. (2007). Rich and rare - first insights into species diversity and abundance of Antarctic abyssal Gastropoda (Mollusca). *Deep Sea Res. Part. 2 Top. Stud. Oceanogr.* 54, 1831–1847. doi: 10.1016/j.dsr2.2007.07.010

Schwenk, K., Sand, A., Boersma, M., Brehm, M., Mader, E., Offerhaus, D., et al. (1998). Genetic markers, genealogies and biogeographic patterns in the Cladocera. *Aquat. Ecol.* 32, 37–51. doi: 10.1023/A:1009939901198

Simon, C., Frati, F., Beckenbach, A., Crespi, B., Liu, H., and Flook, P. (1994). Evolution, weighting, and phylogenetic utility of mitochondrial gene sequences and a compilation of conserved polymerase chain reaction primers. *Ann. Entomol. Soc. Am.* 87, 651–701. doi: 10.1093/aesa/87.6.651

Sirenko, B. (2013). *Check-List of Species of Free-Living Invertebrates of the Russian Far Eastern Seas*. St. Petersburg: Russian Academy of Sciences, Zoological Institute.

Spurr, A. R. (1969). A low-viscosity epoxy resin embedding medium for electron microscopy. *J. Ultrastruct. Res.* 26, 31–43. doi: 10.1016/S0022-5320(69)90033-1

Stamatakis, A. (2014). RAxML version 8: a tool for phylogenetic analysis and post-analysis of large phylogenies. *Bioinformatics* 30, 1312–1313. doi: 10.1093/bioinformatics/btu033

Stöger, I., Sigwart, J. D., Kano, Y., Knebelsberger, T., Marshall, B. A., Schwabe, E., et al. (2013). The continuing debate on deep molluscan phylogeny: evidence for Serialia (Mollusca, Monoplacophora plus Polyplacophora). *Biomed Res. Int.* 407072:18. doi: 10.1155/2013/407072

Sukumaran, J., and Knowles, L. L. (2017). Multispecies coalescent delimits structure, not species. *Proc. Natl. Acad. Sci. U.S.A.* 114, 1607–1612. doi: 10.1073/pnas.1607921114

Thiele, J. (1913). Antarktische solenogastren. *Dtsch. Südpolar Expedition 14 Zool.* 6, 35–65.

Todt, C. (2013). Aplacophoran Mollusks-Still Obscure and Difficult? *Am. Malacol. Bull.* 31, 181–187. doi: 10.4003/006.031.0110

Todt, C., and Kocot, K. M. (2014). New records for the solenogaster *Proneomenia sluiteri* (Mollusca) from Icelandic waters and description of *Proneomenia custodiens* sp. n. *Pol. Polar Res.* 35, 291–310. doi: 10.2478/popore-2014-0012

Todt, C., and Salvini-Plawen, L. V. (2003). New Simrothiellidae (Mollusca: Solenogastres) from the Mozambique Channel, Western Indian Ocean. *Veliger* 46, 252–266.

Todt, C., and Wanninger, A. (2010). Of tests, trochs, shells, and spicules: development of the basal mollusk *Wirenia argentea* (Solenogastres) and its bearing on the evolution of trochozoan larval key features. *Front. Zool.* 7:6. doi: 10.1186/1742-9994-7-6

Untergasser, A., Cutcutache, I., Koressaar, T., Ye, J., Faircloth, B. C., Remm, M., et al. (2012). Primer3—new capabilities and interfaces. *Nucelic Acids Res.* 40, e115–e115. doi: 10.1093/nar/gks596

Vinther, J., Sperling, E. A., Briggs, D. E., and Peterson, K. J. (2012). A molecular palaeobiological hypothesis for the origin of aplacophoran molluscs and their derivation from chiton-like ancestors. *Proc. R. Soc. B Biol. Sci.* 279, 1259–1268. doi: 10.1098/rspb.2011.1773

Watling, L., Guinotte, J., Clark, M. R., and Smith, C. R. (2013). A proposed biogeography of the deep ocean floor. *Prog. Oceanogr.* 111, 91–112. doi: 10.1016/j.pocean.2012.11.003

Wilson, N. G., Rouse, G. W., and Giribet, G. (2010). Assessing the molluscan hypothesis Serialia (Monoplacophora plus Polyplacophora) using novel molecular data. *Mol. Phylogenet. Evol.* 54, 187–193. doi: 10.1016/j.ympev.2009.07.028

Yang, Z. H., and Rannala, B. (2010). Bayesian species delimitation using multilocus sequence data. *Proc. Natl. Acad. Sci. U.S.A.* 107, 9264–9269. doi: 10.1073/pnas.0913022107

Zamarro, M., García-Álvarez, O., and Urgorri, V. (2012). Three new species of Pruvotinidae (Mollusca: Solenogastres) from Antarctica and NW Spain. *Helgol. Mar. Res.* 67, 423–443. doi: 10.1007/s10152-012-0333-0

Zardus, J. D., Etter, R. J., Chase, M. R., Rex, M. A., and Boyle, E. E. (2006). Bathymetric and geographic population structure in the pan-Atlantic deep-sea bivalve *Deminucula atacellana* (Schenck, 1939). *Mol. Ecol.* 15, 639–651. doi: 10.1111/j.1365-294X.2005.02832.x

Zenkevitch, L. (1963). *Biology of the Seas of the USSR*. London: George Allen and Unwin Ltd.

Zhang, C., Zhang, D.-X., Zhu, T., and Yang, Z. (2011). Evaluation of a Bayesian coalescent method of species delimitation. *Syst. Biol.* 60, 747–761. doi: 10.1093/sysbio/syr071

Conflict of Interest Statement: The authors declare that the research was conducted in the absence of any commercial or financial relationships that could be construed as a potential conflict of interest.